SOURCE DATA   TRANSPARENT PROCESS

THE EMBO JOURNAL

Identification of ILK as a critical regulator of VEGFR3 signalling and lymphatic vascular growth

Sofia Urner[1,†], Lara Planas-Paz[1,†], Laura Sophie Hilger[1], Carina Henning[1], Anna Branopolski[1,2], Molly Kelly-Goss[3], Lukas Stanczuk[4], Bettina Pitter[5], Eloi Montanez[5], Shayn M Peirce[3], Taija Mäkinen[4] & Eckhard Lammert[1,6,7,*] [ID]

Abstract

Vascular endothelial growth factor receptor-3 (VEGFR3) signalling promotes lymphangiogenesis. While there are many reported mechanisms of VEGFR3 activation, there is little understanding of how VEGFR3 signalling is attenuated to prevent lymphatic vascular overgrowth and ensure proper lymph vessel development. Here, we show that endothelial cell-specific depletion of integrin-linked kinase (ILK) in mouse embryos hyper-activates VEGFR3 signalling and leads to overgrowth of the jugular lymph sacs/primordial thoracic ducts, oedema and embryonic lethality. Lymphatic endothelial cell (LEC)-specific deletion of *Ilk* in adult mice initiates lymphatic vascular expansion in different organs, including cornea, skin and myocardium. Knockdown of *ILK* in human LECs triggers VEGFR3 tyrosine phosphorylation and proliferation. ILK is further found to impede interactions between VEGFR3 and β1 integrin *in vitro* and *in vivo*, and endothelial cell-specific deletion of an *Itgb1* allele rescues the excessive lymphatic vascular growth observed upon ILK depletion. Finally, mechanical stimulation disrupts the assembly of ILK and β1 integrin, releasing the integrin to enable its interaction with VEGFR3. Our data suggest that ILK facilitates mechanically regulated VEGFR3 signalling via controlling its interaction with β1 integrin and thus ensures proper development of lymphatic vessels.

Introduction

The importance of the lymphatic vasculature is demonstrated by its numerous physiological functions, including maintenance of fluid homeostasis, facilitation of immune response and uptake of lipids and vitamins. Moreover, it is involved in pathological conditions such as primary and secondary lymphoedema, obesity development, tumour cell dissemination and growth, reverse cholesterol transport, hypertension, glaucoma, inflammation and regeneration or damage after myocardial infarction (Karkkainen *et al*, 2000; Skobe *et al*, 2001; Harvey *et al*, 2005; Wilting *et al*, 2009; Martel *et al*, 2013; Thomson *et al*, 2014; Huang *et al*, 2015; Klotz *et al*, 2015; Escobedo *et al*, 2016; Gousopoulos *et al*, 2016; Lund *et al*, 2016; Tatin *et al*, 2017; Zhang *et al*, 2018). Growth of lymphatic vessels, known as lymphangiogenesis, is critically regulated by vascular endothelial growth factor receptor-3 (VEGFR3) signalling, also required for normal blood vascular development (Dumont *et al*, 1998; Veikkola *et al*, 2001). However, after blood vessel formation is completed, VEGFR3 expression shifts to lymphatic endothelial cells (LECs), where it is strictly required for the development of the lymphatic vascular system and lymphangiogenesis (Kaipainen *et al*, 1995; Kukk *et al*, 1996; Karkkainen *et al*, 2004). After birth, VEGFR3 is mainly expressed in LECs, but can also be found in vascular endothelial cells during sprouting angiogenesis and in some fenestrated endothelia (Kaipainen *et al*, 1995; Partanen *et al*, 2000; Tammela *et al*, 2008).

VEGFR3 belongs to the family of receptor tyrosine kinases (RTKs), and its signalling can be activated by binding of vascular endothelial growth factor (VEGF)-C or VEGF-D (Joukov *et al*, 1996; Jeltsch *et al*, 1997; Achen *et al*, 1998). In addition, different co-receptors of VEGFR3 have been reported (Yuan *et al*, 2002; Dixelius *et al*, 2003; Alam *et al*, 2004; Favier *et al*, 2006; Nilsson *et al*, 2010; Wang *et al*, 2010; Xu *et al*, 2010). Binding of ligands to the extracellular part of the receptor induces its dimerisation and

1 Institute of Metabolic Physiology, Heinrich Heine University Düsseldorf, Düsseldorf, Germany
2 Division of Cardiology, Pulmonology and Vascular Medicine, Medical Faculty, Heinrich Heine University Düsseldorf, Düsseldorf, Germany
3 Department of Biomedical Engineering, University of Virginia, Charlottesville, VA, USA
4 Department of Immunology, Genetics and Pathology, Uppsala University, Uppsala, Sweden
5 Walter-Brendel-Center of Experimental Medicine, University Hospital, Ludwig-Maximilians-University of Munich, Munich, Germany
6 Institute for Beta Cell Biology, German Diabetes Center (DDZ), Leibniz Center for Diabetes Research at Heinrich Heine University Düsseldorf, Düsseldorf, Germany
7 German Center for Diabetes Research (DZD e.V.), Neuherberg, Germany
   *Corresponding author. Tel: +49 2118114990; E-mail: lammert@hhu.de
   †These authors contributed equally to this work

autophosphorylation. The latter induces recruitment of intracellular proteins and downstream activation of signalling pathways leading to cell survival, migration and proliferation (Makinen *et al*, 2001; Salameh *et al*, 2005).

A novel aspect of lymphatic vascular biology is the role of integrins and mechanical forces in VEGFR3 signalling, lymphatic vascular growth and valve morphogenesis (Wang *et al*, 2001; Bazigou *et al*, 2009; Galvagni *et al*, 2010; Planas-Paz *et al*, 2012; Baeyens *et al*, 2015; Sweet *et al*, 2015; Sabine *et al*, 2016; Choi *et al*, 2017b). Integrins are transmembrane receptors, which bind to extracellular matrix (ECM) components, and are essential for "outside-in" and "inside-out" signalling of the cell, thereby transducing mechanical stimulations. At least 24 unique heterodimers composed of α and β subunits are known today (Hynes, 2002; Humphries *et al*, 2006). However, predominantly β1 integrins have been reported to be involved in lymphatic vascular development and lymphangiogenesis (Huang *et al*, 2000; Okazaki *et al*, 2009; Garmy-Susini *et al*, 2010; Planas-Paz *et al*, 2012). After binding to the ECM, β1 integrin (e.g. as a subunit of the α5β1 integrin, a receptor for fibronectin) interacts with VEGFR3 to induce c-src-dependent VEGFR3 tyrosine phosphorylation (Wang *et al*, 2001; Zhang *et al*, 2005; Galvagni *et al*, 2010). Further, both the fluid flow through a lymphatic vessel and the interstitial fluid pressure mechanically stimulate LECs (as they are attached to the surrounding ECM via integrins or anchoring filaments); these stimuli trigger VEGFR3 phosphorylation and LEC proliferation (Planas-Paz *et al*, 2012; Planas-Paz & Lammert, 2014; Baeyens *et al*, 2015; Sabine *et al*, 2016; Urner *et al*, 2018). Notably, this mechanoinduced VEGFR3 signalling strictly depends on β1 integrin (Planas-Paz *et al*, 2012).

To our knowledge, no study has reported the role of integrin-linked kinase (ILK) in VEGFR3 signalling or lymphatic vascular development. ILK is a cytoplasmic protein known to—directly or indirectly—interact with β1 and β3 integrins (Hannigan *et al*, 1996; Li *et al*, 1999; Pasquet *et al*, 2002), and it has been identified as a kinase (Hannigan *et al*, 1996). However, since mice harbouring mutations within the proposed autophosphorylation site of ILK are viable and phenotypically normal (Lange *et al*, 2009), its most vital function may be to serve as an adaptor protein modulating cell-matrix interactions and downstream signalling (Ghatak *et al*, 2013). ILK is also found as a central component of the ILK/PINCH/parvin (IPP) complex to ensure linkage between integrins and the actin cytoskeleton (Tu *et al*, 2001; Zervas *et al*, 2001; Sakai *et al*, 2003; Vaynberg *et al*, 2018); it either inhibits or increases cell proliferation depending on the tissue (Gkretsi *et al*, 2008; Serrano *et al*, 2013).

In this study, we investigated the specific role of ILK in VEGFR3 signalling of LECs. We found that ILK acts as a cell-autonomous inhibitor of VEGFR3 signalling during embryonic development as well as in the adult. Specifically, deletion of *Ilk* in LECs resulted in increased VEGFR3 phosphorylation and cell proliferation, as well as lymphatic vascular overgrowth in the mouse embryo. Further, we identified ILK as a regulator of lymph vessel expansion in the heart after myocardial infarction as well as in the skin and cornea of adult mice. Mechanistically, we observed increased interaction of VEGFR3 and β1 integrin in the absence of ILK, and genetic rescue experiments showed that ILK regulates VEGFR3 signalling and lymph vessel growth by controlling β1 integrin. Finally, we found that mechanical stimulation of LECs

disrupts the complex of ILK and β1 integrin, reduces expression of α-parvin and enables β1 integrin to better interact with VEGFR3. Our data indicate that ILK facilitates mechanosensitive VEGFR3 signalling and physiologic lymph vessel expansion by controlling β1 integrin-mediated VEGFR3 activation.

Results

ILK is required to control LEC proliferation and prevent lymphatic vascular overgrowth during mouse embryonic development

In order to investigate the role of ILK in lymphatic vascular development, we used *Flk1-Cre* mice to delete *Ilk* in the endothelium of mouse embryos (Sakai *et al*, 2003; Licht *et al*, 2004). In contrast to embryos with heterozygous endothelial cell-specific *Ilk* deletion (referred to as "control"), mouse embryos with homozygous *Ilk* deletion (referred to as "ILK K.O.") died from E13.5 onwards (Appendix Fig S1A). In comparison with control embryos (Fig 1A–D), ILK K.O. embryos were characterised by dorsolateral oedema and head bleeding (Fig 1E). We first analysed the jugular lymph sacs (jls), also called the primordial thoracic ducts (pTD), using lymphatic vessel endothelial hyaluronan receptor-1 (Lyve1) and CD31 staining. The jls/pTDs are the first lymphatic structures forming pairwise in the developing embryo and give rise to the majority of the entire lymphatic vascular network (Wigle & Oliver, 1999; Wigle *et al*, 2002; Srinivasan *et al*, 2007; Yang *et al*, 2012; Hagerling *et al*, 2013). Notably, we observed a profound expansion of the jls/pTD in ILK K.O. embryos compared to control embryos, visible from E13.0 onwards (Fig 1B–D and F–H). At E14.5, the dermal lymphatic vessels in ILK K.O. embryos were also increased in size, and we observed both lymphatic and blood vascular sprouting defects (Appendix Fig S2A–G).

We next quantified the number of LECs (stained for Lyve1 or Prox1 as lymphatic endothelial markers) and their proliferation within the jls/pTD (Fig 1I–L) to determine whether it coincides with the increased size of the jls/pTD. Indeed, the total LEC number of the jls/pTD was significantly increased in ILK K.O. embryos at E13.5 compared to control littermates (Fig 1M and Appendix Fig S3A–F). Consistent with the increased size of the jls/pTD and greater number of LECs, LEC proliferation in ILK K.O. embryos was found to be significantly increased from E13.0 onwards with both phospho-Histone H3 and Ki67 used as markers for proliferation (Figs 1N and EV1A–I and Appendix Fig S4A–I). In contrast, proliferation of blood endothelial cells (BECs) that were previously shown to be affected by *Ilk* deletion (Friedrich *et al*, 2004; Malan *et al*, 2013) was unchanged in the jugular regions of E13.5 ILK K.O. embryos compared to controls (Appendix Fig S5A–O).

To analyse whether ILK is involved in regulating lymphatic vascular growth and LEC proliferation along with other IPP complex members, we deleted *Parva*, the gene for α-parvin, in endothelial cells (referred to as "α-parvin K.O.") (Fraccaroli *et al*, 2015). Both α- and β-parvin were shown to link ILK to the F-actin cytoskeleton (Nikolopoulos & Turner, 2000; Olski *et al*, 2001). In α-parvin K.O. embryos, a higher number of LECs (Fig EV2A–C) and more LEC proliferation (Fig EV2D–F) were observed compared to control littermates, confirming a regulatory role of the IPP
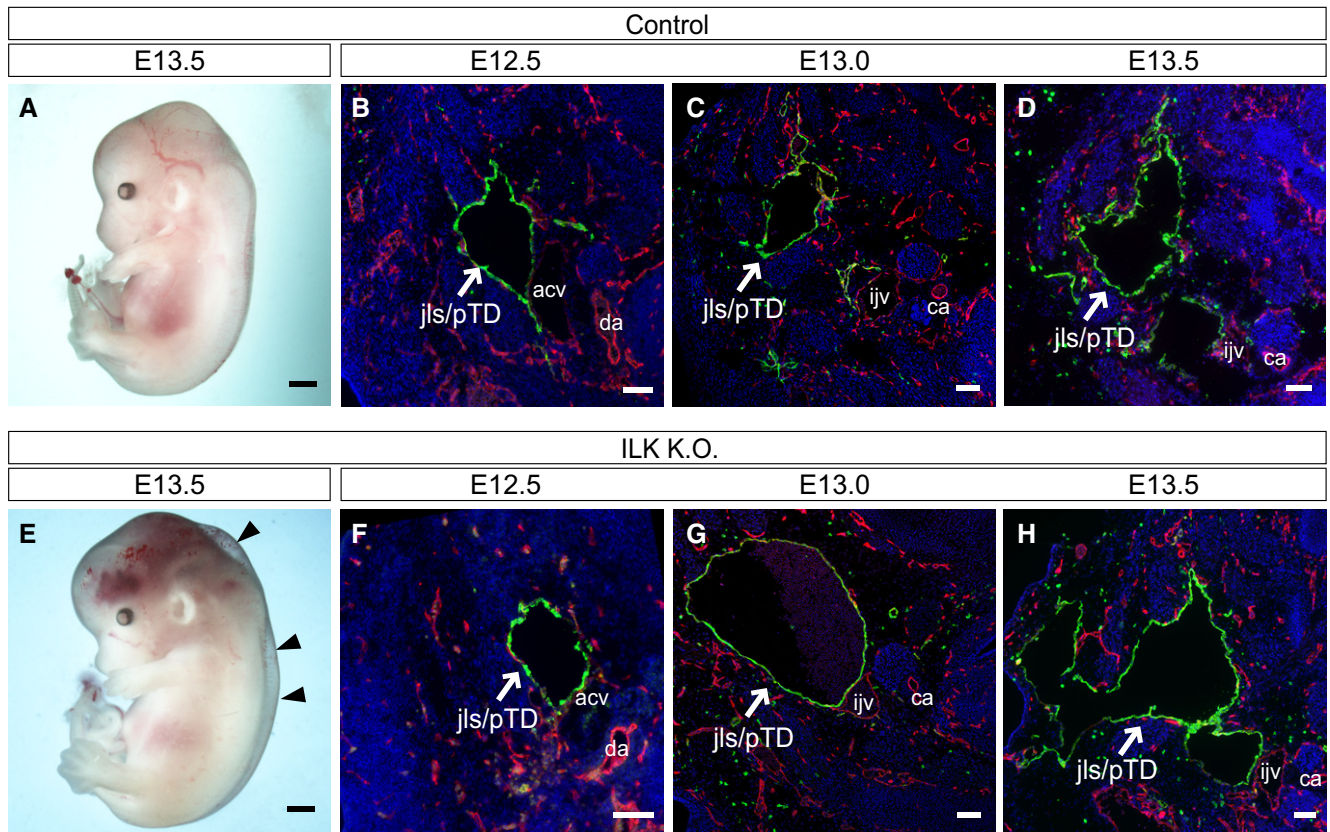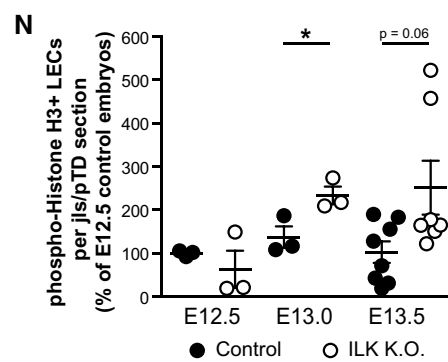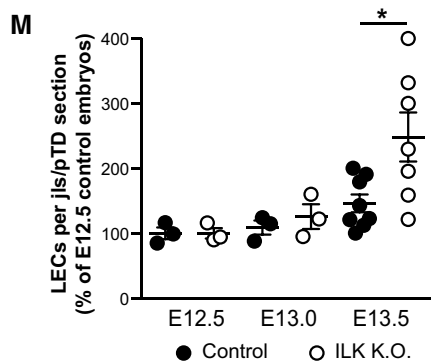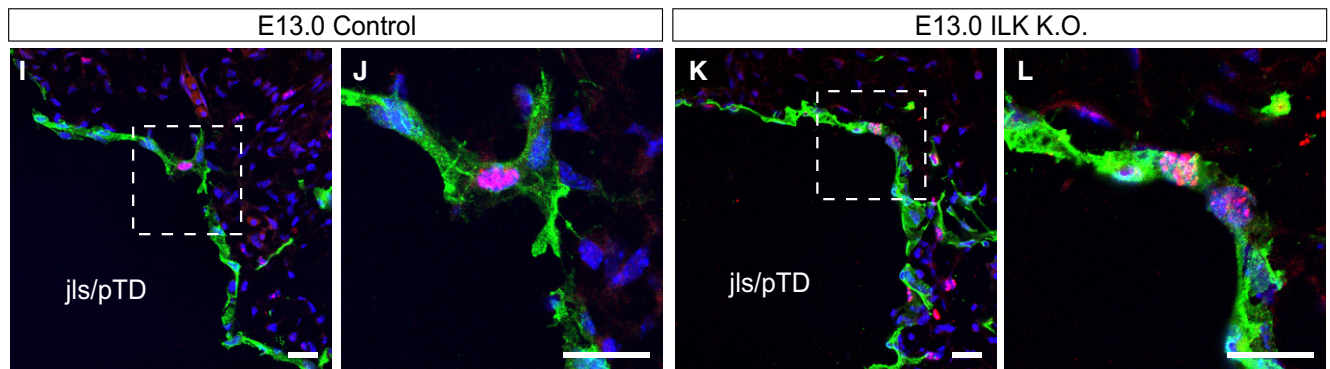
Lyve1 CD31 Nuclei

Figure 1.

Figure 1. ILK controls lymphatic vascular growth in mouse embryos.

A–H E13.5 mouse embryos. (A, E) Bright-field image of a *Flk1-Cre;Ilk*$^{\Delta/+}$ mouse embryo (referred to as "control") with a heterozygous deletion of *Ilk* in endothelial cells and a *Flk1-Cre;Ilk*$^{\Delta/\Delta}$ embryo (referred to as "ILK K.O.") with a homozygous deletion of *Ilk* in endothelial cells. Arrowheads point to oedema. Scale bars: 500 μm. (B–D, F–H) LSM images of cross-sections through control and ILK K.O. embryos at different developmental stages. Arrows point to the jugular lymph sac/primordial thoracic duct (jls/pTD). Anterior cardinal vein (acv), dorsal aorta (da), internal jugular vein (ijv) and carotid artery (ca) are also indicated. Scale bars: 100 μm.

I–L LSM images of cross-sections through the jls/pTD of control or ILK K.O. embryos stained for the proliferation marker phospho-Histone H3. Scale bars: 20 μm.

M Number of LECs per jls/pTD section in control or ILK K.O. embryos (*n* = 3 embryos per genotype at E12.5, E13.0, *n* = 8 control and *n* = 7 ILK K.O. embryos at E13.5), *P* = 0.036.

N LEC proliferation as determined by the number of phospho-Histone H3-positive LECs per jls/pTD section in control or ILK K.O. embryos (*n* = 3 embryos per genotype at E12.5, E13.0, *n* = 8 control and *n* = 7 ILK K.O. embryos at E13.5), *P* = 0.042 (control versus ILK K.O. at E13.0), *P* = 0.058 (control versus ILK K.O. at E13.5).

Data information: Data are presented as means ± SEM, shown as percentage of E12.5 control embryos, unpaired two-tailed Student's *t*-test. Unpaired, two-tailed Mann–Whitney test was additionally performed as a non-parametric test for control versus ILK K.O. at E13.5 in (N), *P* = 0.094.

complex. Finally, we confirmed that the observed effects on LEC proliferation in ILK K.O. embryos are derived from the role of ILK specifically in LECs by restricting *Ilk* deletion to LECs (and LEC progenitors), but not BECs, using the *Prox1-Cre*^{ERT2} promoter (referred to as "induced ILK K.O.", Appendix Fig S1B; Bazigou *et al*, 2011). Consistently, we observed increased LEC proliferation in the jls/pTD of E13.5 induced ILK K.O. embryos compared to controls (Fig EV3A–J).

These results show that ILK, as a member of the IPP complex, is strictly required in LECs to inhibit excessive LEC proliferation and hyperplasia of the lymphatic vasculature during early embryonic development.

ILK controls VEGFR3 signalling during mouse embryonic development

We next analysed *Ilk* gene expression in LECs during different developmental stages of wild-type embryos (referred to as "control", Appendix Fig S6A) along with LEC proliferation (Appendix Fig S6B) and VEGFR3 tyrosine phosphorylation (Appendix Fig S6C). Analysis of mRNA levels suggests an opposite *Ilk* expression pattern compared to both LEC proliferation and VEGFR3 phosphorylation, consistent with the hypothesis that ILK is a negative regulator of LEC proliferation and VEGFR3 activity. Further, the ILK protein could be detected in LECs sorted from mouse embryos at the E13.5 embryonic stage when LEC proliferation and VEGFR3 activation are low compared to earlier embryonic stages (Appendix Fig S6D). We subsequently analysed VEGFR3 signalling in LECs of E13.5 ILK K.O. embryos versus E13.5 control embryos by proximity ligation assays (PLA), in which antibodies against VEGFR3 and phospho-tyrosine were used (Fig 2A–D). Since both VEGFR3 and VEGFR2 are expressed in LECs of the E13.5 jls/pTD (Appendix Fig S7A–H), we also performed a PLA for VEGFR2/p-Tyr (Fig 2E–H). Notably, the average number of VEGFR3/phospho-tyrosine (VEGFR3/p-Tyr) PLA dots was doubled in LECs within the jls/pTD region of E13.5 ILK K.O. embryos compared to controls (Fig 2I), while the PLA for VEGFR2/p-Tyr revealed no significant difference between ILK K.O. and control embryos (Fig 2J and K). Focussing on VEGFR3, we also analysed its activity in *Parva*-deficient embryos, and found VEGFR3 tyrosine phosphorylation to be higher in α-parvin K.O. embryos than in control littermates (Appendix Fig S8A–E), but to a lesser extent than in ILK K.O. embryos (Fig 2I). Finally, we confirmed that also significantly more VEGFR3 activation was observed in induced ILK K.O. embryos, when *Ilk* was deleted from LECs using the *Prox1*

promoter (Fig EV4A–E). Thus, our data indicate that ILK inhibits VEGFR3, but not VEGFR2, signalling in LECs during embryonic development.

### ILK is required to prevent VEGFR3 and β1 integrin interaction in LECs during mouse embryonic development

VEGFR3 tyrosine phosphorylation can be induced by binding of β1 integrin to the ECM (Wang *et al*, 2001; Galvagni *et al*, 2010). Similarly, VEGFR3 is phosphorylated in a β1 integrin-dependent manner upon mechanical stimulation of endothelial cells (Planas-Paz *et al*, 2012; Lorenz *et al*, 2018). As ILK interacts—directly or indirectly—with the intracellular domain of β1 integrin (Hannigan *et al*, 1996; Montanez *et al*, 2008), we first investigated whether either its expression or activation was changed upon ILK depletion in LECs. Integrin activation is associated with conformational changes in the heterodimer that allow interaction and clustering with intracellular signalling molecules, thereby initiating integrin-mediated signalling (reviewed in Avraamides *et al*, 2008). We used antibodies against total and activated β1 integrin on embryonic sections to detect its expression and activity in LECs of the jls/pTD (Appendix Fig S9A–H). However, no major difference in the staining intensity of either total or activated β1 integrin in the LECs of ILK K.O. embryos versus controls was observed at E13.5 (Appendix Fig S9I and J), when VEGFR3 phosphorylation and LEC proliferation differed between these embryos.

Next, since VEGFR3 phosphorylation involves physical interaction between VEGFR3 and β1 integrin (Wang *et al*, 2001; Zhang *et al*, 2005; Planas-Paz *et al*, 2012; Lorenz *et al*, 2018), and since both proteins appear to partially colocalise on the plasma membrane of LECs (Fig 3A–D), we investigated whether ILK depletion results in altered interactions between VEGFR3 and β1 integrin. Notably, the analysis of VEGFR3/β1 integrin PLA dots in LECs of the jls/pTD revealed a significantly higher number of interactions in E13.5 ILK K.O. embryos versus control embryos (Fig 3E–I). Therefore, the presence of ILK attenuates interactions between VEGFR3 and β1 integrin, thereby inhibiting non-physiologic hyper-activation of VEGFR3 signalling.
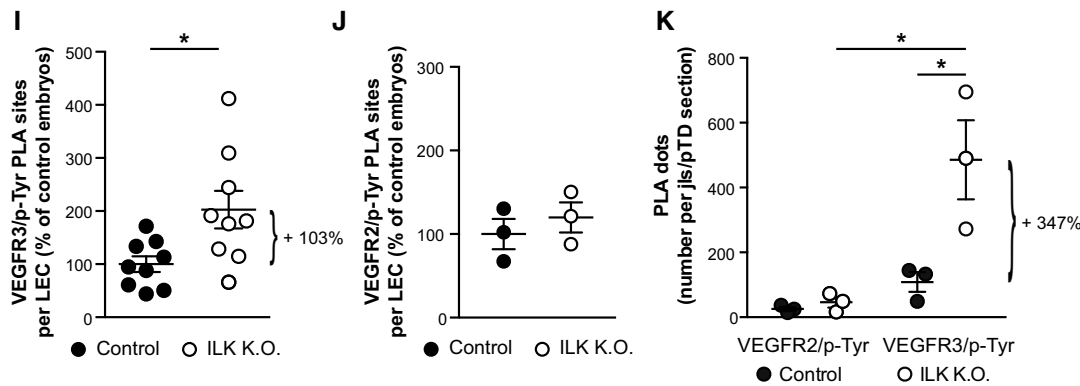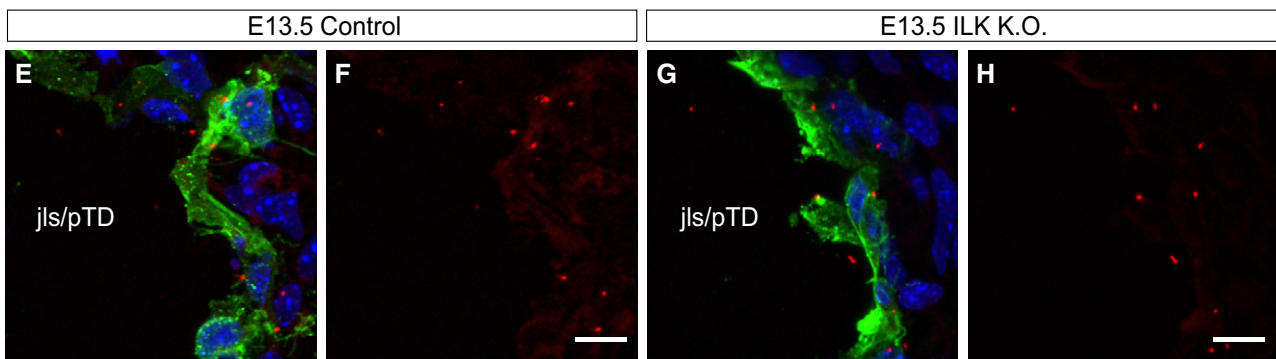
The regulatory role of ILK in lymphatic vascular growth depends on β1 integrin

In a previous study, we found that endothelial cell-specific deletion of *Itgb1* results in strongly reduced VEGFR3 phosphorylation,

Lyve1 VEGFR3/p-Tyr PLA Nuclei
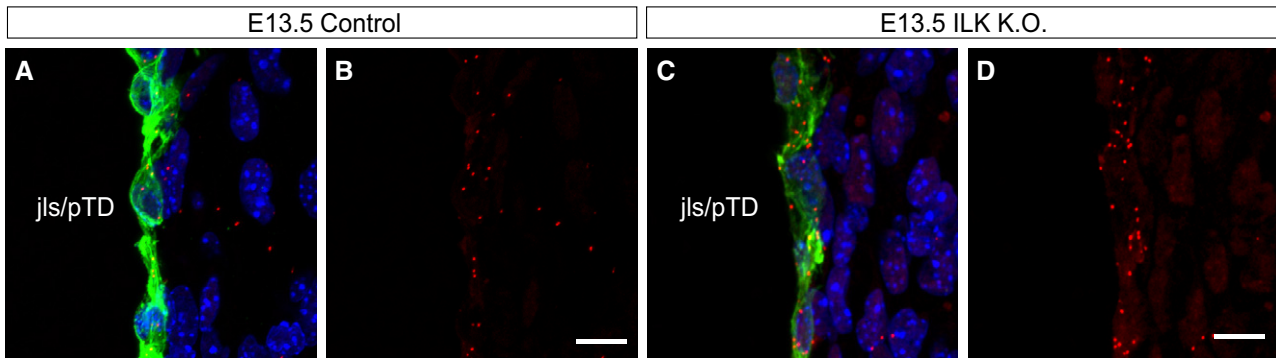
Lyve1 VEGFR2/p-Tyr PLA Nuclei

Figure 2. ILK controls tyrosine phosphorylation of VEGFR3 in mouse embryos.

A–D   LSM images of proximity ligation assay (PLA) dots composed of VEGFR3 and phosphorylated tyrosine (p-Tyr) on cross-sections through the jugular lymph sac/
        primordial thoracic duct (jls/pTD) of E13.5 control and ILK K.O. embryos. Scale bars: 10 μm.
E–H   LSM images of PLA dots composed of VEGFR2 and phosphorylated tyrosine (p-Tyr) on cross-sections through the jls/pTD of E13.5 control and ILK K.O. embryos.
        Scale bars: 10 μm.
I   Quantification of the PLA dots indicating VEGFR3 with phosphorylated tyrosine (p-Tyr) per LEC of E13.5 control or ILK K.O. embryos (n = 9 embryos per genotype),
   *P = 0.022.
J   Quantification of the PLA dots indicating VEGFR2 with phosphorylated tyrosine (p-Tyr) per LEC of E13.5 control or ILK K.O. embryos (n = 3 embryos per genotype).
K   Quantification of the total number of PLA dots indicating both VEGFR2 (left) and VEGFR3 (right) with phosphorylated tyrosine (p-Tyr) per jls/pTD section of E13.5
        control or ILK K.O. embryos (n = 3 embryos per genotype), *P = 0.005 (VEGFR2/p-Tyr in ILK K.O. versus VEGFR3/p-Tyr in ILK K.O.), *P = 0.013 (VEGFR3/p-Tyr in
        control versus VEGFR3/p-Tyr in ILK K.O.).

Data information: Data are presented as means ± SEM, and in (I, J) data are shown as percentage of control embryos; unpaired two-tailed Student's *t*-test (I, J) or two-
way ANOVA with Tukey's multiple comparisons test (K). Note that not all significances are shown in (K).

decreased LEC proliferation and a lower LEC number, as well as significantly smaller jls/pTD during embryonic development (Planas-Paz *et al*, 2012). In contrast, we observed the exact opposite phenotype in ILK K.O. embryos for all mentioned criteria (Figs 1

and 2). Since we found β1 integrin to interact more with VEGFR3 in the absence of ILK (Fig 3), we deleted an *Itgb1* allele to test whether reduced β1 integrin expression restores physiologic lymphatic vascular growth in *Ilk*-deficient mouse embryos (Fig 4). Specifically,

Surface VEGFR3 β1 integrin Nuclei
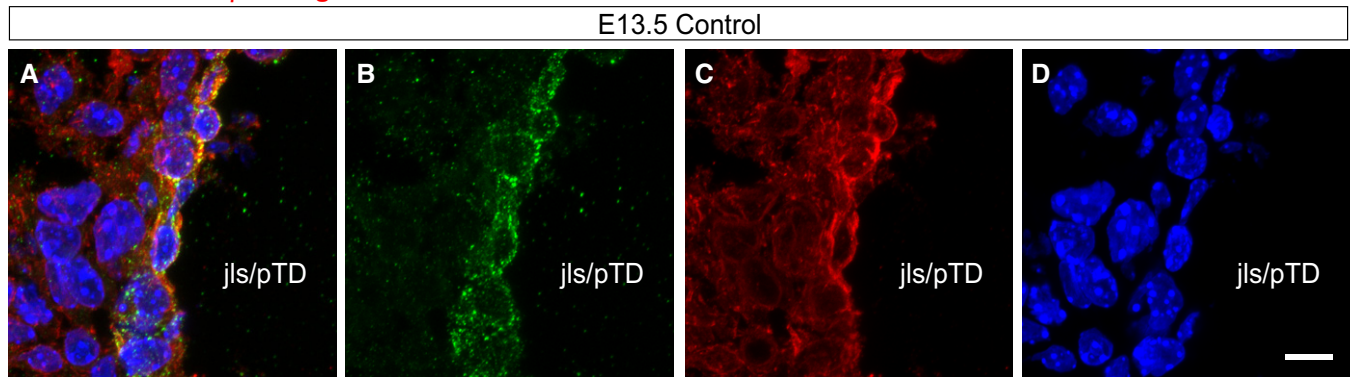
Lyve1 VEGFR3/β1 integrin PLA Nuclei
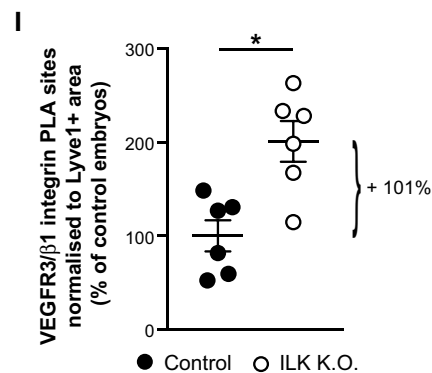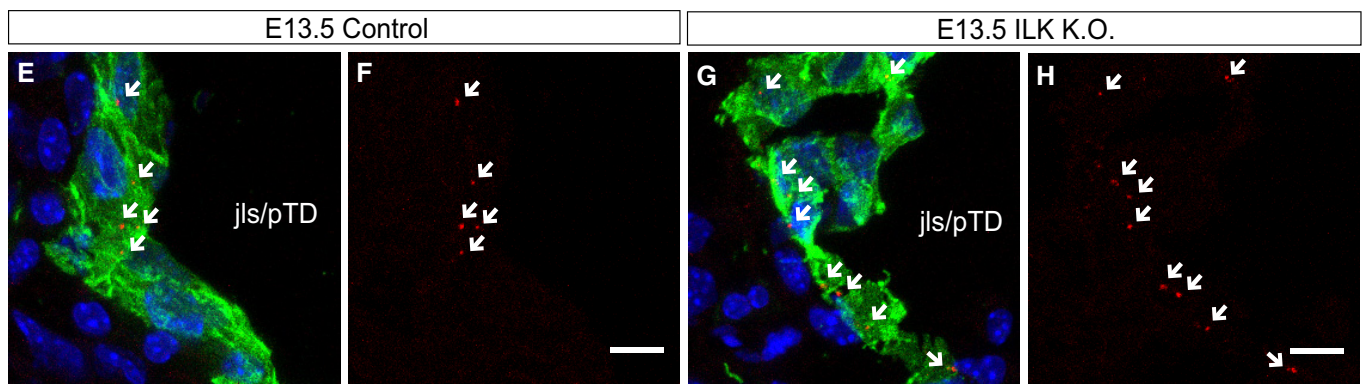
Figure 3.   ILK controls VEGFR3-β1 integrin interactions in mouse embryos.

A–D   LSM images of cross-sections through the jugular lymph sac/primordial thoracic duct (jls/pTD) of an E13.5 control embryo stained for surface VEGFR3 and β1 integrin. Scale bar: 10 μm.

E–H   LSM images of proximity ligation assay (PLA) dots (arrows) composed of VEGFR3 and β1 integrin on cross-sections through the jls/pTD of E13.5 control and ILK K.O. embryos. Scale bars: 10 μm.
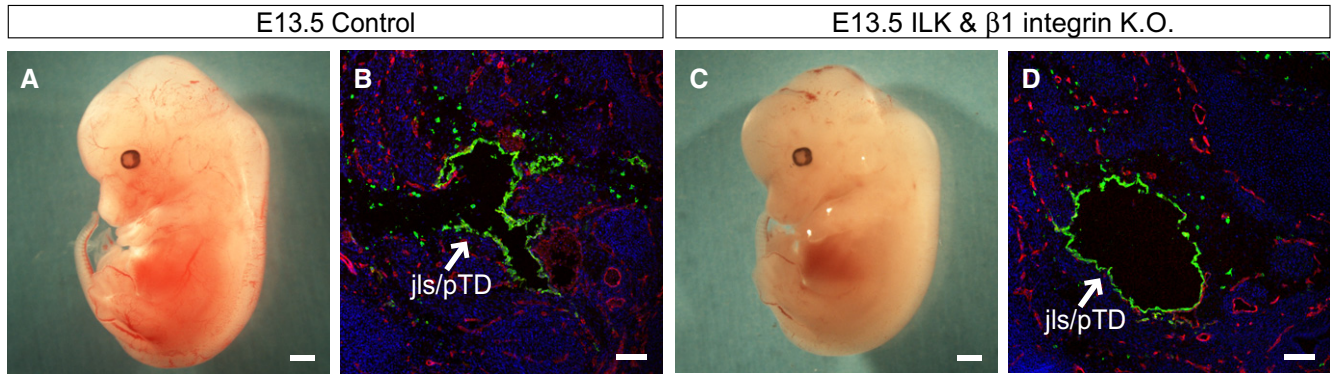
I   Quantification of VEGFR3/β1 integrin PLA dots normalised to Lyve1-positive area of control or ILK K.O. embryos (*n* = 6 embryos per genotype), *P = 0.005.

Data information: Data are presented as means ± SEM, shown as percentage of control embryos, unpaired two-tailed Student's *t*-test.
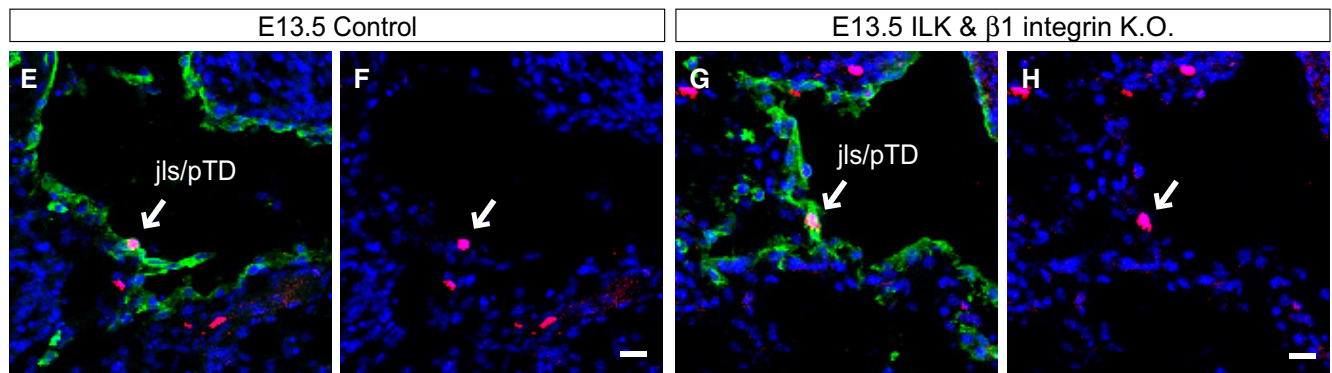
we compared E13.5 embryos with heterozygous deletion of both *Itgb1* and *Ilk* (referred to as "control", Fig 4A and B) with embryos with heterozygous *Itgb1* and homozygous *Ilk* deletion (referred to as "ILK & β1 integrin K.O.", Fig 4C and D). Even though more ILK & β1 integrin K.O. embryos died compared to ILK K.O. embryos, fewer embryos had oedema or haemorrhages (Appendix Fig S1A and C).

Analysis of the jls/pTD size by quantification of the total LEC number as well as LEC proliferation, as indicated by phospho-Histone H3 staining (Fig 4E–H), and VEGFR3 phosphorylation, as detected by PLA for VEGFR3/p-Tyr (Fig 4I–L), revealed no difference between control and ILK & β1 integrin K.O. embryos (Fig 4M–O), indicating a genetic rescue of the lymphatic vascular

Figure 4.

phenotype in all analysed parameters. These results suggest that the regulatory effect of ILK on VEGFR3 signalling, LEC proliferation and lymphatic vascular growth strictly depends on β1 integrin.

ILK is required to control lymphatic vascular growth in the adult mouse

To determine whether ILK also regulates VEGFR3 signalling and LEC proliferation in the adult lymphatic vasculature, we used adult *Prox1-Cre*^{ERT2} mice to delete *Ilk* specifically in LECs (Fig 5; Bazigou *et al*, 2011). We analysed the lymphatic vascular density of the ear skin 2 weeks after the last tamoxifen injection (Fig 5A–D), as well as LEC proliferation (Fig 5E–H) and VEGFR3 phosphorylation as early as 2 days after the last tamoxifen injection. Thereby, we observed a significant increase in the dermal lymph vessel density of *Prox1-Cre*^{ERT2}*;Ilk*$^{\Delta/\Delta}$ mice (referred to as "adult ILK K.O.") compared to *Prox1-Cre*^{ERT2}*;Ilk*$^{+/+}$ mice (referred to as "adult control") (Fig 5I). In addition, a significant increase in the number of proliferating LECs in dermal lymphatic vessels of adult ILK K.O. mice was detected (Fig 5J), and an ELISA for tyrosine-phosphorylated VEGFR3 indicated a doubled VEGFR3 tyrosine phosphorylation in skin lysates of adult ILK K.O. mice compared to adult controls (Fig 5K). Next, we investigated the effect of *Ilk* deletion on an avascular tissue by analysing the cornea of adult ILK K.O. mice. Strikingly, we found a significantly higher number of lymphatic vessels protruding into the cornea of adult ILK K.O. mice compared to adult controls around 6 weeks after the last tamoxifen injection (Fig 5L–N). Therefore, even in adult mice, *Ilk* deletion increases VEGFR3 signalling, LEC proliferation and lymphatic vascular growth.

ILK regulates lymphatic vascular growth after myocardial infarction (MI)

Recently published studies revealed the importance of the cardiac lymphatic vasculature and its remodelling during the recovery phase after myocardial infarction (MI) (Ishikawa *et al*, 2007; Klotz *et al*, 2015; Henri *et al*, 2016; Tatin *et al*, 2017). Notably, the importance of ILK in cardiomyocytes and in regulating cardiac function was previously reported by several publications (Bendig *et al*, 2006; Lu *et al*, 2006; White *et al*, 2006; Ding *et al*, 2009; Gu *et al*, 2012; Traister *et al*, 2012). ILK protein is expressed in LECs sorted from the adult mouse heart (Appendix Fig S6D); however, to our knowledge, the function of ILK in cardiac lymphatic vessels has not yet been analysed. We therefore used adult ILK K.O. mice to first analyse the lymphatic vasculature in the heart 2 weeks after the last tamoxifen injection (Fig 6A–D). While we observed a significant upregulation of the cardiac lymph vessel density by 39% (*$P = 0.019$) within lateral regions of the ventricles (Fig 6A and B), we only saw a non-significant increase when quantifying the lymph vessel density in total heart sections (Fig 6C), while the blood vessel density was virtually unchanged (Fig 6D). The data suggest that ILK regulates lymphatic vascular growth in the adult myocardium, but its regulatory strength might depend on the location of lymphatic vessels, which were recently described to be anatomically and morphologically heterogeneous in the heart (Norman & Riley, 2016; Tatin *et al*, 2017).

Next, we analysed the cardiac lymph vessel density in adult ILK K.O. mice versus control mice after MI. Two weeks after the last tamoxifen injections, the mice underwent an occlusion of the left
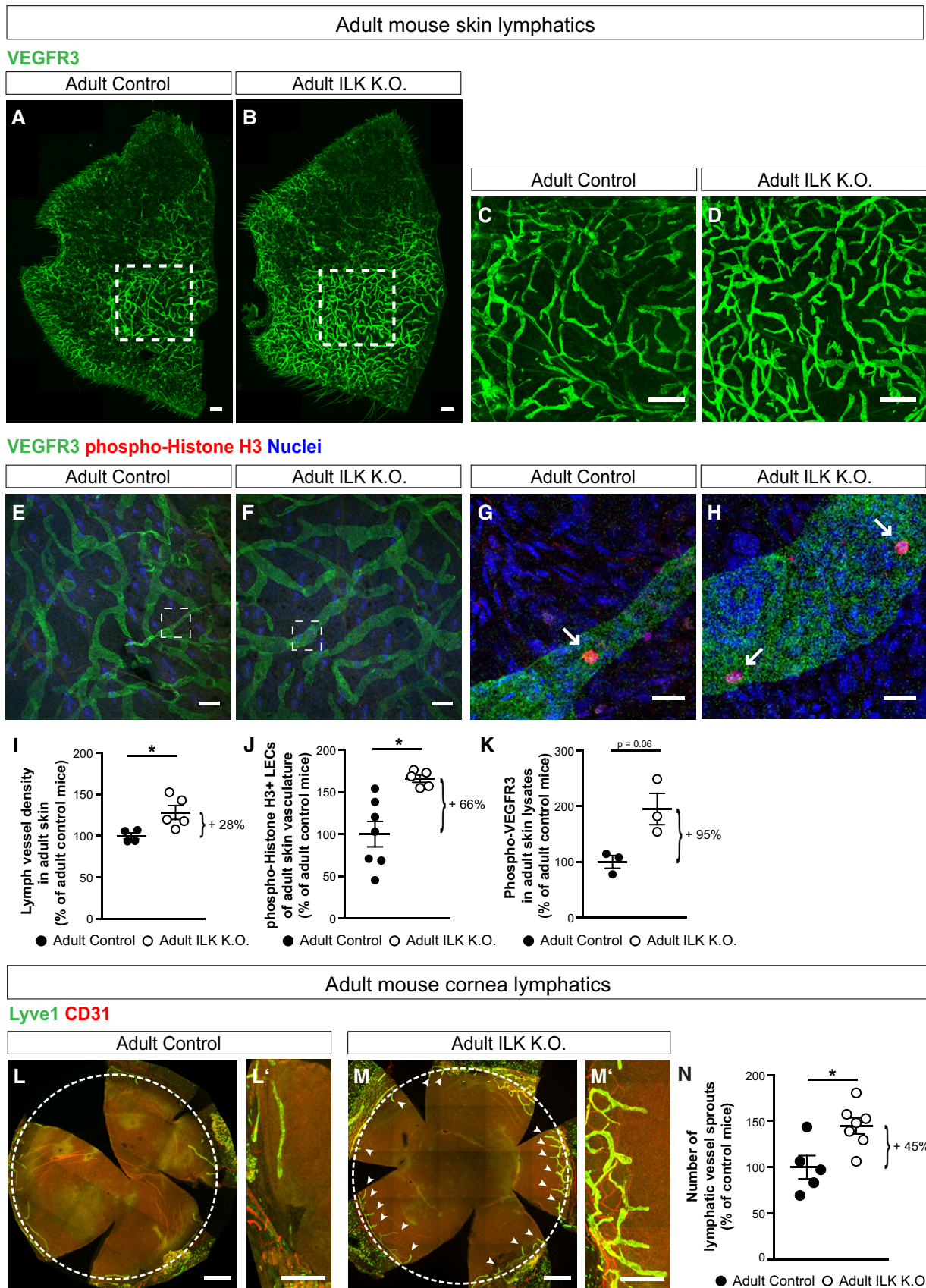
Figure 5.

anterior descending coronary artery (LAD) for 60 min, resulting in myocardial ischaemia, followed by reperfusion of the LAD (Fig 6E–H) (Nossuli *et al*, 2000). Around 4 weeks after MI, adult ILK K.O. mice revealed a higher cardiac lymph vessel density compared to that of control mice, while the cardiac blood vessel density was lower (Fig 6G and H). Notably, the fraction of CD68-positive macrophages in the Lyve1-positive area was unchanged in ILK K.O. versus control mice and only accounted for around 1% of the total cardiac Lyve1-positive area after MI (Appendix Fig S10A–I). These observations suggest that ILK controls cardiac lymph vessel density after MI.

ILK controls LEC proliferation, VEGFR3 signalling and interactions between VEGFR3 and β1 integrin in adult human LECs

Finally, we aimed to reproduce our results on ILK in the human system. Therefore, we transfected primary human LECs with either a control siRNA (referred to as "control") or one of three different siRNAs against *ILK* (referred to as "ILK-1", "ILK-2" and "ILK-3") and analysed the knockdown (KD) efficiency at both the mRNA and protein level (Appendix Fig S11). *ILK* mRNA levels were reduced by up to 85% (Appendix Fig S11A), while ILK protein was downregulated by up to 80% (Appendix Fig S11B and C). Next, we performed BrdU incorporation assays to analyse LEC proliferation upon ILK KD (Fig 7A–C). Consistent with our *in vivo* results, we observed significantly increased proliferation in human LECs upon ILK KD (Fig 7C). Analysis of VEGFR3 phosphorylation in human LEC lysates was performed by ELISA and showed a significantly increased tyrosine phosphorylation of human VEGFR3 when *ILK* was silenced (Fig 7D). Further, we performed PLA experiments with human LECs to analyse interactions between VEGFR3 and β1 integrin. In line with the *in vivo* data, we observed an increased number of PLA dots (normalised to the number of analysed LECs) upon silencing of *ILK* (Fig 7E–G).

Mechanical stretch of adult human LECs results in dissociation of ILK from β1 integrin and reduced expression of α-parvin

Recently, we found that mechanotransduction in LECs results in enhanced VEGFR3 signalling and LEC proliferation in a β1 integrin-dependent manner *in vivo* and *in vitro* (Planas-Paz *et al*, 2012). To show that mechanical stimulation of LECs leads to interaction of β1 integrin and VEGFR3 (Planas-Paz *et al*, 2012), similar to ILK depletion, adult human LECs were mechanically

stretched and subsequently analysed for VEGFR3/β1 integrin interaction. Notably, significantly more VEGFR3/β1 integrin PLA dots were detected in mechanically stretched versus unstretched LECs (Fig 8A–E). Next, we analysed the effect of mechanical stimulation on the interaction between ILK and β1 integrin by co-immunoprecipitation (Co-IP) assays, in which we used HA-tagged β1 integrin for IP with subsequent detection of ILK in the IP lysates via Western blotting (Fig 8F, G). The anti-HA antibody selectively precipitated β1 integrin compared to the IgG control antibody, and more ILK protein was found to be precipitated using anti-HA antibodies compared to control IgG antibodies (Appendix Fig S12A–C). Even though only small amounts of ILK could be precipitated with HA-tagged β1 integrin, we observed a significant reduction in ILK protein associated with β1 integrin in LEC lysates after mechanical stimulation (Fig 8G).

We next analysed the effect of mechanical stretching on the expression of ILK and α-parvin protein, and found no substantial reduction in ILK protein levels upon stretching human LECs (Appendix Fig S12D and E). In contrast, protein levels of α-parvin (as an F-actin binding protein of the IPP complex) were significantly reduced (Appendix Fig S12F). Similar to the mechanical stimulation, knockdown of *ILK* significantly reduced α-parvin protein levels (Fig EV5A–C), whereas *PARVA* knockdown did not substantially affect ILK protein expression (Fig EV5D–F), suggesting ILK is upstream of α-parvin. The results indicate that in the absence of mechanical stimulation, the assembly of ILK (as part of the IPP complex) and β1 integrin attenuates the interaction of β1 integrin with VEGFR3 and thus prevents non-physiologic VEGFR3 activation and LEC proliferation.

Discussion

VEGFR3 is a highly mechanoresponsive RTK (Planas-Paz *et al*, 2012; Baeyens *et al*, 2015; Coon *et al*, 2015; Choi *et al*, 2017a; Lorenz *et al*, 2018), and β1 integrin is critically required for full VEGFR3 activation (Wang *et al*, 2001; Galvagni *et al*, 2010; Planas-Paz *et al*, 2012). Surprisingly, we identified ILK and β1 integrin to have opposing roles in VEGFR3 signalling and lymphatic vascular growth. Based on our genetic, cell biological and biochemical results we obtained using primary human LECs, as well as embryonic and adult mice, we propose a novel molecular mechanism of how β1 integrin-mediated VEGFR3 signalling is regulated endogenously in order to prevent excessive lymphatic

---

Figure 6. ILK controls lymphatic vascular growth in the heart after myocardial infarction.

A, B　LSM images of cross-sections through the heart of an adult *Prox1-Cre*[ERT2]*;Ilk*^{+/+} mouse (referred to as "adult control") and *Prox1-Cre*[ERT2]*;Ilk*[Δ/Δ] mouse (referred to as "adult ILK K.O.") showing the outer lateral region of the left ventricle (LV). Scale bars: 100 μm.

C, D　Overall cardiac lymph vessel and blood vessel density in heart sections as determined by Lyve1-positive and CD31-positive area (normalised to total analysed myocardial area), respectively (*n* = 4 control and *n* = 5 ILK K.O. mice).

E, F　LSM images of cross-sections through the heart of an adult control and ILK K.O. mouse 4 weeks after myocardial ischaemia and reperfusion (MI/R), showing the outer lateral region of the LV. Scale bars: 100 μm.

G, H　Overall cardiac lymph vessel and blood vessel density in heart sections as determined by Lyve1-positive and CD31-positive area (normalised to total analysed myocardial area), respectively (*n* = 5 control and *n* = 7 ILK K.O. mice), *P* = 0.051 (cardiac lymph vessel density in adult control or adult ILK K.O.), **P* = 0.025 (cardiac blood vessel density in adult control or adult ILK K.O.).

Data information: Data are presented as means ± SEM, shown as percentage of control mice, unpaired two-tailed Student's *t*-test.

▶
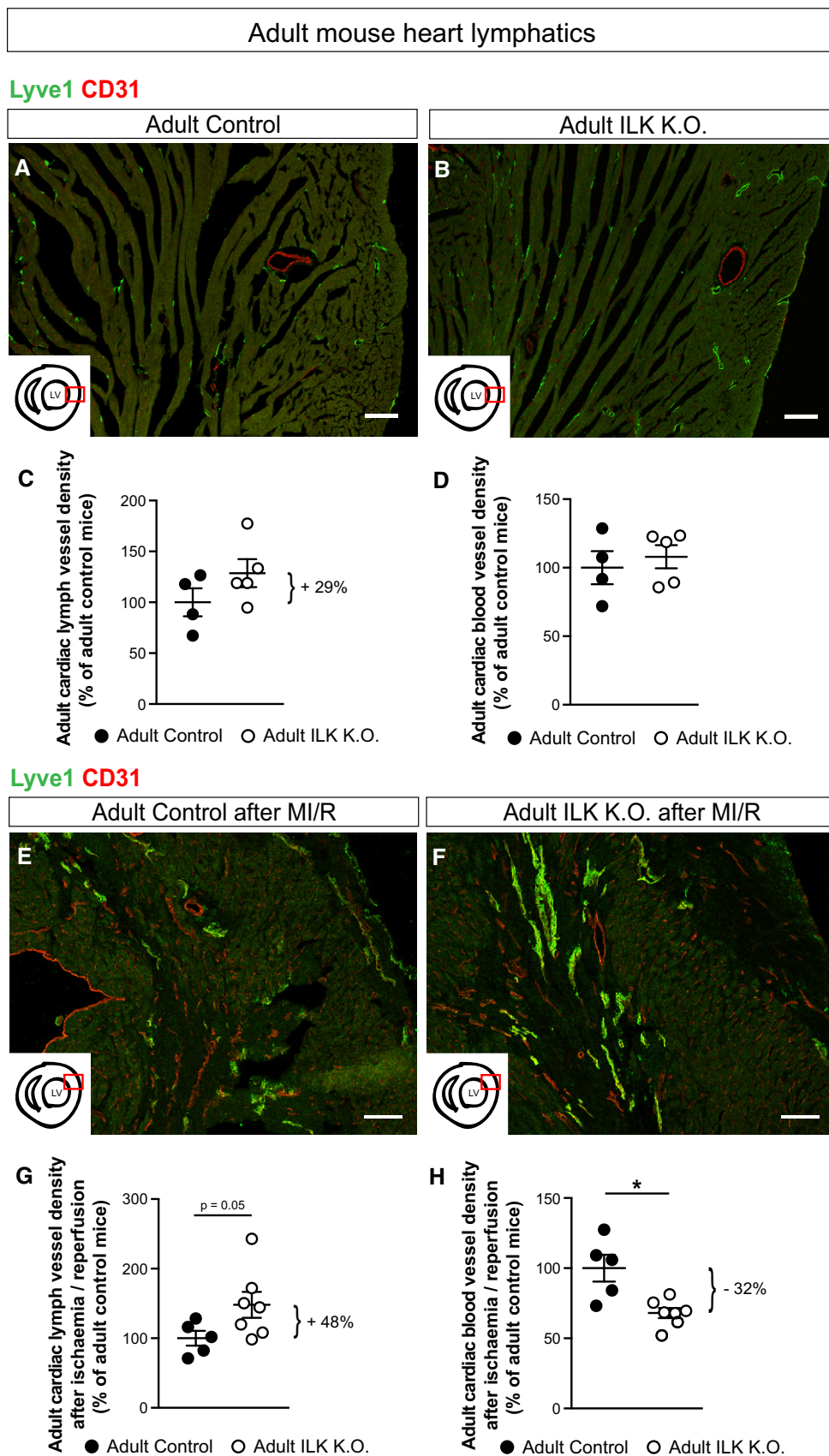
Figure 6.
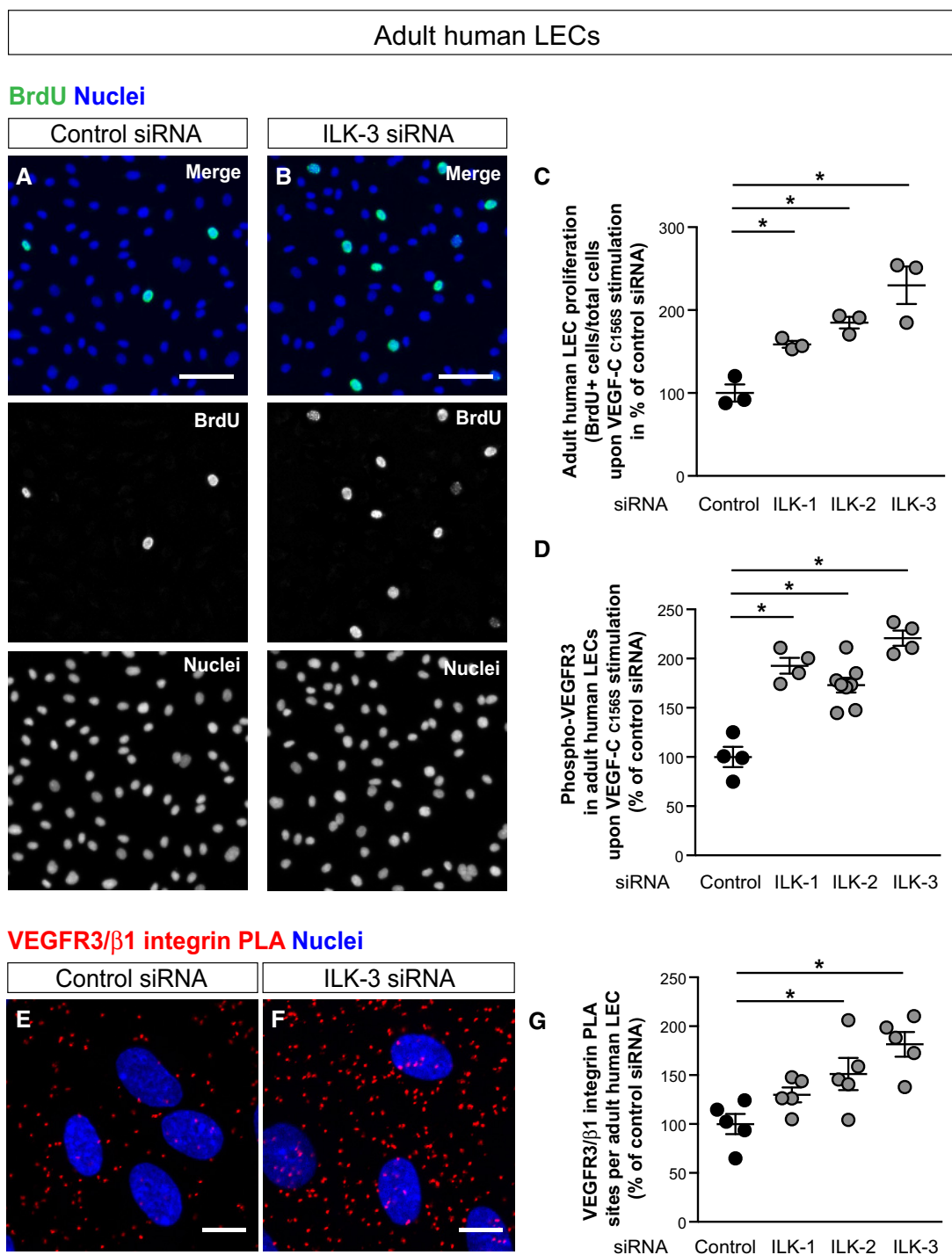
Figure 7. ILK controls proliferation, VEGFR3 signalling and VEGFR3-β1 integrin interactions in human LECs.

A, B   Images of adult human LECs after 1 h of BrdU incorporation and previous transfections with control or ILK siRNA. Scale bars: 50 μm.

C   LEC proliferation as determined by the number of BrdU-positive cells normalised to the total number of LECs previously transfected with control siRNA or ILK siRNAs in the presence of VEGF-C Cys156Ser (n = 3 independent transfections per siRNA), *P = 0.032 (control versus ILK-1), *P = 0.005 (control versus ILK-2), *P = 0.0003 (control versus ILK-3).

D   VEGFR3 tyrosine phosphorylation as determined by ELISA of lysates from adult human LECs transfected with control siRNA or ILK siRNAs in the presence of VEGF-C Cys156Ser (n = 4 (control siRNA, ILK-1 siRNA and ILK-3 siRNA) or n = 8 (ILK-2 siRNA) independent transfections per siRNA), *P = 0.0001 (control versus each siRNA).

E, F   LSM images of VEGFR3/β1 integrin PLA dots in human LECs transfected with control or ILK siRNA. Scale bars: 10 μm.

G   Quantification of VEGFR3/β1 integrin PLA dots per human LEC after transfection with control siRNA or ILK siRNAs (n = 5 independent transfections per siRNA), P = 0.234 (control versus ILK-1), *P = 0.024 (control versus ILK-2), *P = 0.001 (control versus ILK-3).

Data information: Data are presented as means ± SEM, shown as percentage of control siRNA, one-way ANOVA with Dunnett's multiple comparisons test.
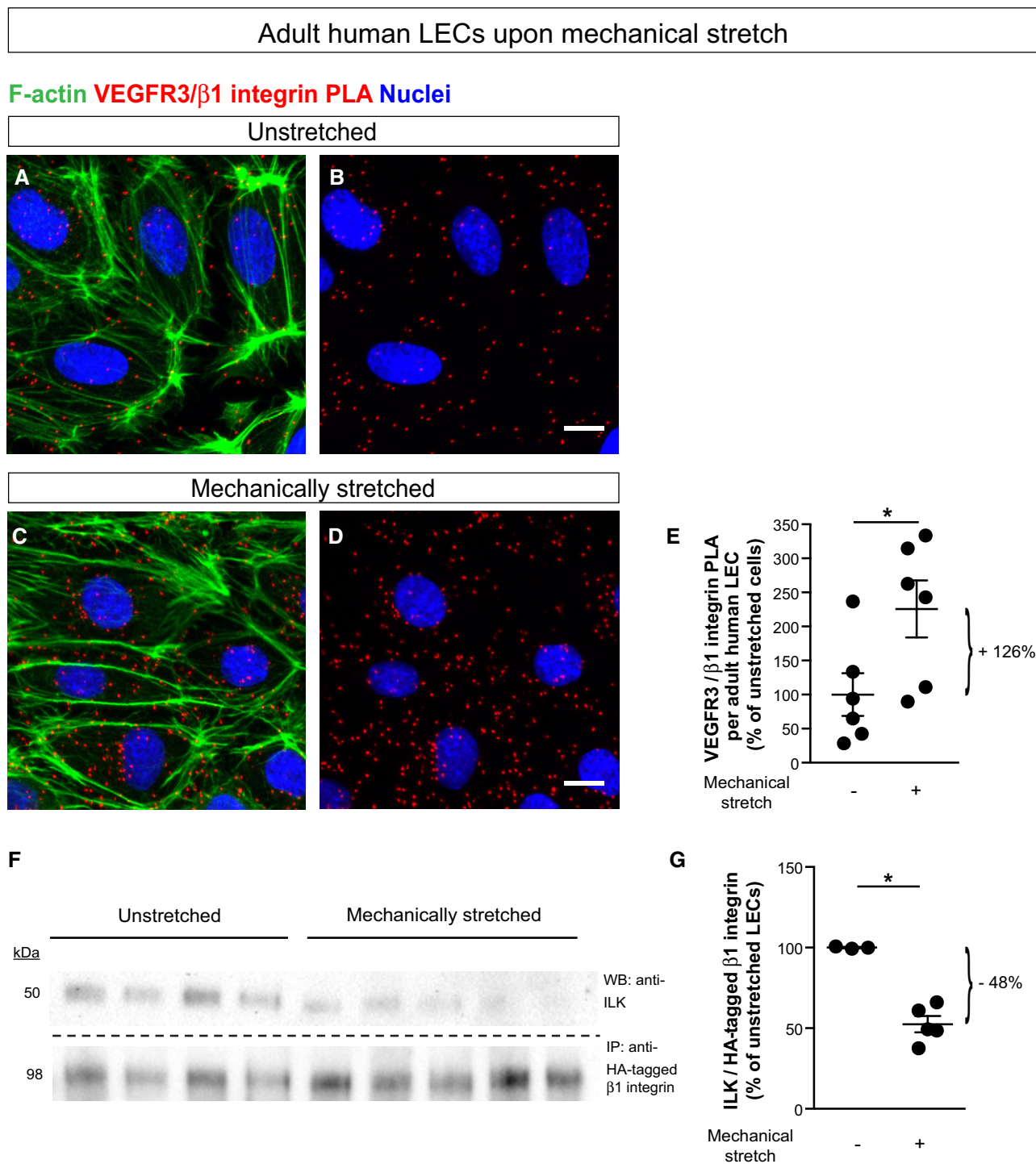
Figure 8. Mechanically stretched human LECs have more VEGFR3-β1 integrin and less ILK-β1 integrin interactions.

A–D   LSM images of PLA dots in human LECs that were kept unstretched or mechanically stretched for 30 min. Red dots are PLA dots composed of VEGFR3 and β1 integrin. Scale bars: 10 μm.

E   Quantification of VEGFR3/β1 integrin PLA dots per human LEC with (+) or without (−) mechanical stretch (*n* = 6 independent stretch chambers), *P = 0.039.

F   Western blot (WB) image of human LECs that were either kept unstretched or stretched for 30 min and used for immunoprecipitation (IP) of HA-tagged β1 integrin from whole cell lysates with subsequent detection of interacting ILK in IP lysates.

G   Quantification of the ILK protein amount in IP lysates from LECs with (+) or without (−) mechanical stretch; normalised to the respective amount of HA-tagged β1 integrin (*n* = 3 (unstretched) or *n* = 5 (stretched) independent stretch chambers), *P = 0.0007.

Data information: Data are presented as means ± SEM, unpaired two-tailed Student's *t*-test.
Source data are available online for this figure.

vascular growth (Fig 9). In the absence of mechanical stimulation, ILK attenuates interaction between VEGFR3 and β1 integrin, likely with other IPP complex members, such as α-parvin (Fig 9A), which was shown to be one of the strongest interaction partners of ILK (Dobreva *et al*, 2008), and is known to interact with the F-actin cytoskeleton (Nikolopoulos & Turner, 2000; Olski *et al*, 2001). The interaction between ILK and β1 integrin may be direct or indirect (e.g. via Kindlin-2) (Hannigan *et al*, 1996; Montanez *et al*, 2008; Horton *et al*, 2015; Kadry *et al*, 2018). Upon mechanical stimulation of LECs—such as during increased interstitial fluid accumulation when the LECs are stretched—ILK dissociates from β1 integrin (Fig 9B), thereby facilitating the interaction of β1 integrin with VEGFR3 (Fig 9C). This molecular interaction increases VEGFR3 tyrosine phosphorylation, LEC proliferation and lymphatic vascular growth (Planas-Paz *et al*, 2012). Notably, similar to mechanical stimulation, loss of ILK

results in increased interaction between VEGFR3 and β1 integrin, reduced α-parvin expression and leads to strongly upregulated VEGFR3 signalling, as well as LEC proliferation, causing lymphatic vascular growth (Fig 9D).

Lymphatic network formation requires a careful balance of pro- and anti-lymphangiogenic regulators (reviewed by Schulte-Merker *et al*, 2011; Klein & Caron, 2015; Sabine *et al*, 2016). Disturbing this balance leads to hypo- or hyperplasia of lymphatic vessels, which is of clinical importance across multiple pathologies (Rutkowski *et al*, 2006; Klotz *et al*, 2015; Gousopoulos *et al*, 2016, 2017; Henri *et al*, 2016; Tatin *et al*, 2017). Here, we identified ILK to be required to limit VEGFR3 signalling and lymphatic vascular growth in developmental, physiological and pathological conditions. Without ILK, the lymphatic vasculature undergoes excessive growth, which is rescued by decreasing the expression of β1 integrin. Thus, via "hijacking" β1 integrin and keeping it away from
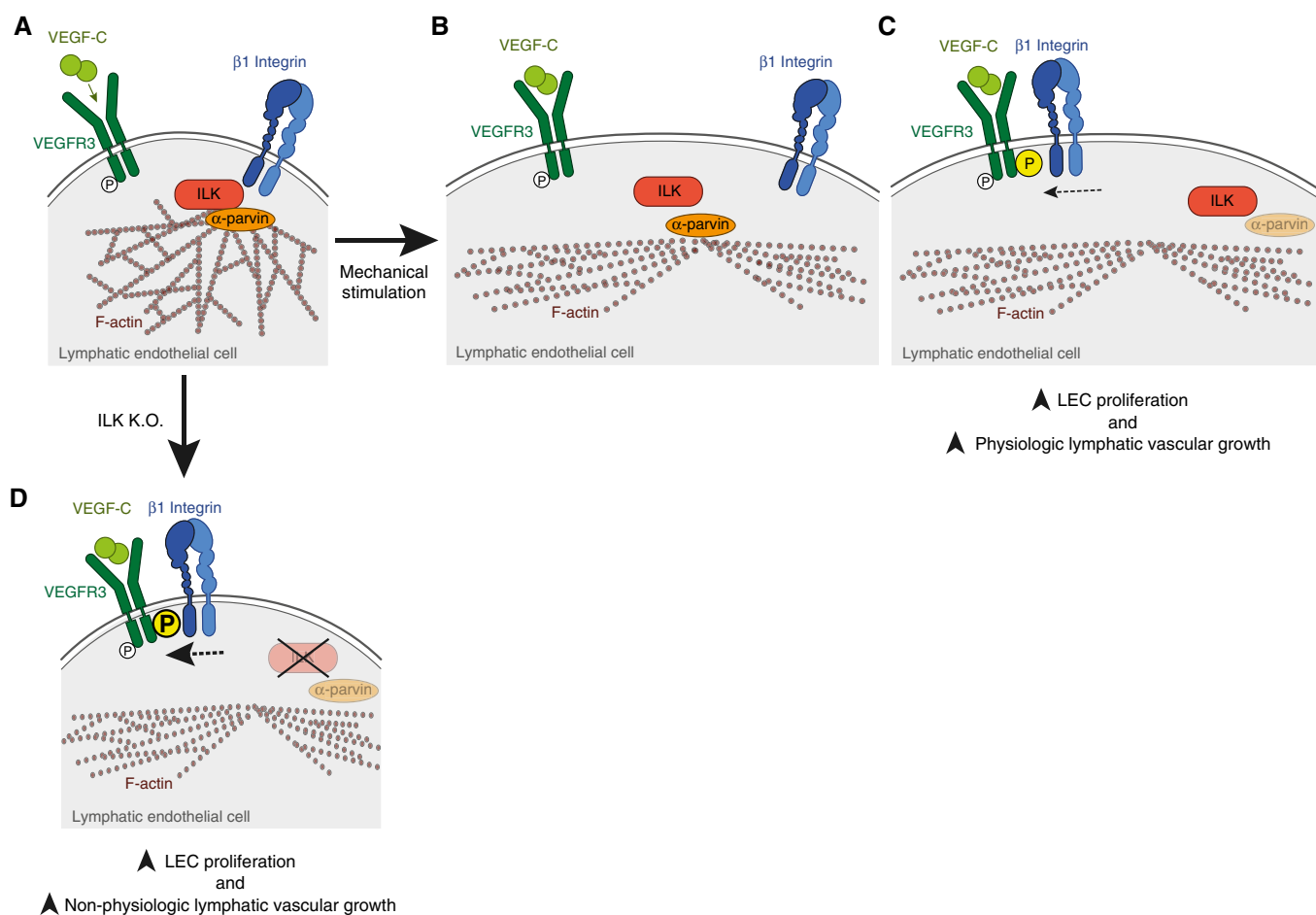
Figure 9. Simplified model of mechanosensitive VEGFR3 signalling and ILK-controlled lymphatic vascular growth.

A   In quiescent LECs, VEGFR3 and β1 integrin are physically separated. ILK directly or indirectly interacts with β1 integrin and connects it to the F-actin cytoskeleton via intracellular proteins, such as α-parvin, a component of the IPP complex.

B   Upon mechanical stretch, the complex of β1 integrin and ILK (along with the entire IPP complex) transiently disrupts.

C   This releases β1 integrin, resulting in its interaction with VEGFR3, and thus in increased VEGFR3 tyrosine phosphorylation ("P" in yellow circle). As a consequence, LEC proliferation and lymphatic vascular growth are induced.

D   The absence of ILK results in permanent interaction between VEGFR3 and β1 integrin, leading to upregulated VEGFR3 tyrosine phosphorylation ("P" in yellow circle), LEC proliferation and non-physiologic lymphatic vascular growth.

VEGFR3, ILK facilitates translation of mechanical cues into cellular responses (Fig 9A–C), which are essential for the controlled development of a stable, appropriately sized lymphatic vascular network.

Materials and Methods

Mice

C57Bl/6J (Janvier) mouse embryos were used for wild-type studies. *Flk1-Cre* mice and *Ilk-loxP* mice have been separately described previously (Sakai *et al*, 2003; Licht *et al*, 2004). For additional genetic deletion of *Itgb1*, these mice were crossed with *Itgb1-loxP* mice (Potocnik *et al*, 2000). For lymphatic endothelial cell (LEC)-specific deletion of *Ilk*, we used *Prox1-Cre^{ERT2}* mice (Bazigou *et al*, 2011). Embryos with endothelial cell-specific *Parva* deletion were generated by crossings of *Tie2-Cre* mice (Kisanuki *et al*, 2001) and *Parva-loxP* mice (Montanez *et al*, 2009; Fraccaroli *et al*, 2015). In general, littermates or mouse embryos with a similar genetic background served as controls. Adult female *Prox1-Cre^{ERT2}* mice and *Ilk-loxP* mice at the age of 15–25 weeks (age-matched within each experiment) were used to analyse the effect of *Ilk* deletion in LECs. To induce Cre-mediated recombination in *Prox1-Cre^{ERT2}* and *Prox1-Cre^{ERT2};Ilk-loxP* embryos, pregnant mice were given intraperitoneal tamoxifen (Sigma, T5648, solved in peanut oil) injections (40 mg/kg) for two consecutive days at the embryonic stage E11.0 and E12.0, while adult mice were given six consecutive tamoxifen injections (40 mg/kg). Adult tissues were collected and analysed 2 days, 2 or 6 weeks after the last tamoxifen injection, as indicated in the results.

Myocardial infarction

For the induction of myocardial ischaemia, *Prox1-Cre^{ERT2}* and *Prox1-Cre^{ERT2};Ilk-loxP* mice were subjected to a temporary ligation of the left anterior descending coronary artery (LAD) for 60 min, followed by reperfusion. For the surgical procedures, a closed-chest model was chosen to reduce inflammatory reactions that are due to the surgical trauma itself (Nossuli *et al*, 2000). Therefore, mice underwent a pre-surgery 1 week after the last tamoxifen injection, in which the suture was placed underneath the LAD, in principle following the detailed protocol described in Merx *et al* (2014). Briefly, mice were anesthetised by intraperitoneal injections of ketamine (100 mg/kg bodyweight, Ketanest® S, Pfizer Pharma GmbH) and xylazine (10 mg/kg bodyweight, Rompun™, Bayer Healthcare), followed by respiration with isoflurane (2.0 vol.%, Piramal Healthcare). A 7-0 surgical suture (Ethicon, Johnson and Johnson) was carefully passed underneath the LAD at a position around 1 mm from the tip of the left auricle, and the ends of the suture were threaded through a PE tubing and placed in the subcutaneous tissue pocket. Ligation of the LAD to induce myocardial ischaemia was performed 1 week after the pre-surgery. Therefore, mice were re-anesthetised with isoflurane (3.0 vol.%), the skin was opened, and ischaemia was induced by gently pulling the suture ends affixed to metal picks apart until ST elevation was seen on the electrocardiography (ECG). 60 min later, reperfusion was confirmed by resolution of ST elevation. Mice were harvested around 4 weeks after MI and used for analyses of the cardiac lymphatic vasculature, as well as for corneal lymphangiogenesis studies.

Magnetic-activated cell sorting

Whole mouse hearts or jugular regions of mouse embryos were isolated and immediately dissociated using the gentleMACS™ Dissociator (Miltenyi Biotec), as described in Planas-Paz *et al* (2012) and the customer protocol by Miltenyi Biotec ("Isolation of lymphatic endothelial cells (LECs) from mouse embryos using the gentleMACS™ Dissociator"). Briefly, cell suspensions were labelled with rat anti-mouse PECAM-1-FITC clone 390 (Millipore, CBL1337F) and rabbit anti-mouse Lyve-1 (Abcam, ab14917) antibodies or goat anti-mouse Lyve-1 (R&D Systems, AF2125) antibodies that were previously conjugated to magnetic Microbeads using the MACSflex MicroBead Kit according to the manufacturer's protocol (Miltenyi Biotec, 130-105-805). LECs were sorted in a stepwise manner using anti-FITC MultiSort microbeads (Miltenyi Biotec, 130-058-701), followed by goat anti-rabbit IgG microbeads (Miltenyi Biotec, 130-048-602) or self-conjugated goat anti-Lyve1 microbeads (R&D Systems, AF2125; Miltenyi Biotec, 130-105-805). Subsequently, sorted LECs were either homogenised with peqGold TriFast (Peqlab) for quantitative real-time PCR or frozen for Western blotting.

Immunohistochemistry of embryonic sections

Embryos were fixed in 4% PFA (Chemsolute, TH. Geyer) overnight (at 4°C), stepwise cryopreserved in 15 and 30% sucrose (Sigma) overnight (at 4°C), embedded in Tissue Tek O.C.T. embedding media (Thermo Fisher Scientific) and transversally separated into 12-μm cryosections. Specifically, all sections from beginning of the embryonic neck region to the beginning of the heart were collected consecutively on SuperFrost slides (Thermo Fisher Scientific), so that the whole jugular lymph sacs/primordial thoracic ducts (jls/pTD) region was present on each slide. For quantification of total LEC numbers per jls/pTD section, only sections of centrally located, lumenised jls/pTD were analysed, while LEC proliferation was determined by counting proliferating LECs on sections through the entire jls/pTD regions. Quantification of total LECs or proliferating LECs was subsequently normalised to the number of analysed sections. Proliferation of blood vascular endothelial cells (BECs) was quantified in the embryonic region around the jls/pTD and normalised to the DAPI-positive area. The following antibodies were used for immunostainings: goat anti-mouse Lyve-1 (R&D Systems, AF2125), rabbit anti-mouse Lyve-1 (Abcam, ab14917), goat anti-human Prox1 (R&D, AF2727), goat anti-mouse VEGFR3 (R&D Systems, AF743), rabbit anti-mouse VEGFR2 clone 55B11 (Cell Signaling, 2479), rat anti-mouse CD31/PECAM-1 (BD Bioscience, 553370), rabbit anti-phospho-Histone H3 (Millipore, 06-570), rabbit anti-Ki67 (Merck Millipore, AB9260) and rat anti-activated β1 integrin clone 9EG7 (BD Bioscience, 553715). For surface VEGFR3/β1 integrin staining, fixed mouse embryonic sections were incubated with goat anti-mouse VEGFR3 antibody (R&D Systems, AF743) without any detergent, while they were washed thoroughly afterwards, and incubated with rat anti-β1 integrin clone MB1.2 (Merck Millipore, MAB1997) in the presence of detergent (0.2% Triton X-100, AppliChem). Secondary

antibodies conjugated with AF488, AF555 (Molecular Probes), Cy3 or Cy5 (Jackson ImmunoResearch) were used. DAPI (Sigma) was used to counterstain cell nuclei. All images were acquired using Laser Scan Microscopy (LSM 710, Zeiss) and analysed using the ImageJ software.

Immunohistochemistry of adult mouse sections

Adult mouse hearts were fixed in 4% PFA (Chemsolute, TH. Geyer) overnight (at 4°C), stepwise cryopreserved in 15 and 30% sucrose (Sigma) overnight (at 4°C), embedded in Tissue Tek O.C.T. embedding media (Thermo Fisher Scientific) and transversally separated into consecutive 12-μm cryosections on SuperFrost slides (Thermo Fisher Scientific). The following antibodies were used for immunostaining: goat anti-mouse Lyve-1 (R&D Systems, AF2125), rabbit anti-mouse Lyve1 (Abcam, ab14917), rat anti-mouse CD31/PECAM-1 (BD Bioscience, 553370), goat anti-CD31 (R&D Systems, AF3628), rabbit anti-Prox1 (Proteintech, 11067-2-AP) and rat anti-CD68 (Invitrogen, 14-0681-82). Secondary antibodies conjugated with AF488 (Molecular Probes), Cy3 or Cy5 (Jackson ImmunoResearch) were used. DAPI (Sigma) was used to counterstain cell nuclei. All images were acquired using Laser Scan Microscopy (LSM 710, Zeiss) and analysed using the ImageJ software.

Whole-mount staining of embryonic and adult mouse tissues

For whole-mount staining, whole embryos were fixed in 4% PFA (Chemsolute, TH. Geyer) overnight (at 4°C), and skins were gently removed. Adult mouse ears were collected and tissue layers gently separated. The inner ear layer was fixed in 4% PFA (Chemsolute, TH. Geyer) overnight (at 4°C), and the internal-facing side was imaged. For corneal lymphangiogenesis analyses, mouse corneas were collected and fixed in acetone (VWR) for 20 min (at RT). The following antibodies were used for whole-mount stainings: goat anti-mouse VEGFR3 (R&D Systems, AF743), rabbit anti-phospho-Histone H3 (Millipore, 06-570), goat anti-Lyve1 (R&D Systems, AF2125) and rat biotin anti-mouse CD31 (BioLegend, 102504). Secondary antibodies conjugated with AF488 (Molecular Probes) or Cy3 (Jackson ImmunoResearch) were used. DAPI (Sigma) was used to counterstain cell nuclei. All images were acquired using Laser Scan Microscopy (LSM 710, Zeiss) and analysed using the ImageJ software. Quantification of the dermal lymph vessel size in mouse embryos was performed by determining Lyve1-positive area with exclusion of macrophages and normalisation to the number of lymph vessels per image. For analysis of dermal lymph vessel densities in adult mice, a tile scan of the whole ear skin was performed; the central region was subsequently analysed for VEGFR3-positive area, which was normalised to the total analysed area. For analysis of proliferating LECs in the skin, the number of phospho-Histone H3-positive cells was normalised to the VEGFR3-positive area per image. For corneal lymphangiogenesis studies, a tile scan of the whole mouse cornea was performed, and the total number of lymphatic vascular sprouts protruding into the cornea was counted.

Cell culture and transfections

All *in vitro* experiments were performed with adult human dermal microvascular lymphatic endothelial cells (LECs) (Promocell or

Lonza). These cells were not found in the database of commonly misidentified cell lines that are maintained by ICLAC and NCBI BioSample. Cells were authenticated by stimulation with 100 ng/ml VEGF-C Cys156Ser (R&D Systems) and subsequent detection of VEGFR3 phosphorylation. Cells were also tested negative for mycoplasma contamination. For experiments, LECs were grown in endothelial cell growth medium MV2 (Promocell or Lonza) and used at passages ≤ P6. All cell culture dishes were coated with fibronectin (2.5 μg/cm², human plasma fibronectin purified protein, Millipore).

Cell stretch studies were performed by growing cells on STREX stretch chambers (BioCat, ST-CH-04-BR) for 24 or 48 h, and then stretching them for 30, 60 or 120 min (Planas-Paz *et al*, 2012). Afterwards, cells were either immediately fixed in 4% PFA and used for proximity ligation assays or lysed for co-immunoprecipitation assays or Western blotting.

To achieve an *ILK* knockdown, cells were transfected with 250–500 nM stealth siRNAs against human ILK (Invitrogen): ILK-1 5′-GCCUGUGGCUGGACAACACGGAGAA-3′, ILK-2 5′-CAGCCAGUCAU GGACACCGUGAUAU-3′ and ILK-3 5′GCAUUGACUUCAAACAGCUU AACUU-3′, or non-targeting control siRNAs (Invitrogen) with a similar GC content, and incubated for 48–72 h. To achieve a *PARVA* knockdown, cells were transfected with 150 nM stealth siRNAs against human α-parvin (Invitrogen): PARVA-1 5′-CAAGCUGAAU GUGGUGAAA-3′, PARVA-2 5′-CCUGAAAUCUACACUACGA-3′ and PARVA-3 5′-GAACUGAUGAAGGUAUUAA-3′, or non-targeting control siRNAs (Invitrogen) with a similar GC content, and incubated for 48 h. For analysis of knockdown efficiencies, quantitative real-time PCR or Western blotting was performed. For co-immunoprecipitation assays, LECs were transfected with 1 μg C-terminally human influenza hemagglutinin (HA)-tagged β1 integrin plasmid (Sino Biological, HG10587-CY) and subsequently cultured on stretch chambers. All transfections were performed using the Nucleofec-tor™ 2b Device or the 4D-Nucleofector™ System (Lonza).

Co-immunoprecipitation (Co-IP) and Western blotting

48 hours after HA-tagged β1 integrin plasmid transfection, LECs were stretched for 30 min and subsequently collected in ice-cold lysis buffer containing 50 mM HEPES pH 7.0, 150 mM NaCl, 10% glycerol, 1% Triton X-100, 1 mM activated Na_3VO_4, phosphatase inhibitors (Phosphatase Inhibitor Cocktail, Roche or Sigma-Aldrich) and protease inhibitors (cOmplete, Protease Inhibitor Cocktail Tablets, Roche). Protein concentrations were determined by using the Pierce™ BCA Protein Assay (Thermo Fisher Scientific). Equal amounts of protein (200-300 μg) were used for a pre-clearing step (1 h at 4°C) of the lysates with 30 μl Protein G Plus/Protein A Agarose Suspension (Millipore, IP05-1.5 ml). For immunoprecipitation, pre-cleared lysates were incubated with 3 μl rabbit anti-HA tag antibody (Cell Signaling, 3724) or equal concentration of normal rabbit IgG (Cell Signaling, 2729) overnight (at 4°C), followed by another incubation with 30 μl Protein G Plus/Protein A Agarose Suspension for 3 h (at 4°C). After supernatants were removed, beads were washed with IP lysis buffer, and samples were analysed via Western blotting. In general, Western blotting was performed for Co-IP analyses, determination of knockdown efficiencies or protein levels after cell stretch studies, as well as for analysis of MACS-sorted LECs. Therefore, samples

were collected in Laemmli buffer containing 10 mM NaF, 1 mM activated Na_3VO_4, protease inhibitors (complete, Protease Inhibitor Cocktail Tablets, Roche), phosphatase inhibitors (Phosphatase Inhibitor Cocktail, Sigma-Aldrich), 1x Laemmli (Bio-Rad) and 1% 2-Mercaptoethanol (Roth). The Invitrogen Novex Mini-Cell Device (Thermo Fisher Scientific) or the Mini-PROTEAN® Tetra Cell Device (Bio-Rad) was used for protein separation. For Western blotting, the Trans-Blot Turbo Transfer System (Bio-Rad) and following antibodies were used: rabbit anti-ILK (Cell Signaling, 3862), rabbit anti-α-parvin (Cell Signaling, 4026) and rabbit anti-GAPDH (Abcam, ab9485) for the determination of knockdown efficiencies or cell stretch studies, rabbit anti-HA tag (Cell Signaling, 3724) and mouse anti-ILK (BD Biosciences, 611803) for Co-IP studies and rabbit anti-Prox1 (Proteintech, 11067-2-AP) and rabbit anti-ILK (Cell Signaling, 3862) for analysis of MACSed LECs. Normal rabbit IgG (Cell Signaling, 2729) was used as control in IPs and Western blots. *ILK* and *PARVA* knockdown efficiencies after siRNA transfections were determined by normalisation of ILK or α-parvin protein amount to their respective GAPDH protein amount, while the amount of ILK protein detected in the IP lysates was normalised to the respective HA-tagged β1 integrin protein amount during quantification.

In vitro proliferation assay

To analyse human LEC proliferation, cells were starved overnight in basal medium without growth factors (EBM-2 MV, Promocell or Lonza), washed with PBS and incubated with 100 ng/ml VEGF-C Cys156Ser (R&D Systems) and 10 μM 5-bromo-2′-deoxyuridine (BrdU, Sigma) for 1 h. Cells were washed with PBS, immediately fixed in ethanol fixative (70% ethanol, 30% glycine 50 nM), and staining was performed with mouse anti-BrdU antibody (BD Bioscience, 555627). Secondary antibody conjugated with AF488 (Molecular probes) was used, as was DAPI (Sigma) to counterstain cell nuclei. Imaging was performed by using fluorescence microscopy (Nikon Eclipse Ti-S) and analysed with the ImageJ software. For analysis of proliferating human LECs, 10 images were taken from cells per transfection, and the number of BrdU-positive cells was divided by the total cell number to determine proliferation rates.

ELISA

To determine VEGFR3 phosphorylation in mouse skin lysates, ears were collected and the inner ear layer was immediately homogenised in ice-cold lysis buffer containing 50 mM HEPES pH 7.0, 150 mM NaCl, 10% glycerol, 1% Triton X-100, 1 mM activated Na_3VO_4, phosphatase inhibitors (Phosphatase Inhibitor Cocktail, Roche or Sigma-Aldrich) and protease inhibitors (cOmplete, Protease Inhibitor Cocktail Tablets, Roche). For analysis of human VEGFR3 phosphorylation, cells were starved overnight in basal medium without growth factors (EBM-2 MV, Promocell or Lonza), washed with PBS and stimulated for 5 min with 100 ng/ml VEGF-C Cys156Ser (R&D Systems). After washing in PBS, cells were immediately lysed in the same ice-cold lysis buffer. Protein concentrations were determined by using the Pierce™ BCA Protein Assay (Thermo Fisher Scientific). Equal amounts of protein were loaded on the ELISA. VEGFR3 phosphorylation was detected by using the DuoSet

IC human phospho-VEGFR3 ELISA (R&D Systems) according to the manufacturer's protocol. In addition, tissue lysates were normalised to total VEGFR3 amounts using the DuoSet IC human total VEGFR3 ELISA (R&D Systems).

Proximity ligation assay

Proximity ligation assays were performed to determine tyrosine phosphorylation of VEGFRs or protein interactions (Soderberg *et al*, 2006) according to the manufacturer's protocol using the Duolink *in situ* reagents (Olink Bioscience). The following antibodies were used on embryonic sections: goat anti-mouse VEGFR3 (R&D Systems, AF743), rabbit anti-mouse VEGFR2 clone 55B11 (Cell Signaling, 2479), mouse anti-phospho-tyrosine 4G10 Platinum (Millipore, 05-1050) and rat anti-mouse β1 integrin clone MB1.2 (Millipore, MAB1997). The following antibodies were used for *in vitro* PLA studies: goat anti-human VEGFR3 (R&D Systems, AF349) and mouse anti-human β1 integrin (Millipore, MAB1987). Co-stainings were performed using rabbit anti-mouse Lyve-1 (Abcam, ab14917) or Alexa Fluor®488 phalloidin (Invitrogen by Thermo Fisher, A12379). Secondary antibodies conjugated with AF488 (Molecular Probes) were used, as well as DAPI (Sigma) to counterstain cell nuclei. All images were acquired using Laser Scan Microscopy (LSM 710, Zeiss) and analysed using the ImageJ software. PLA dots were normalised to the number of LECs or to the Lyve1-positive area.

Quantitative real-time PCR

Total RNA was isolated using the phenol/chloroform extraction method (Chomczynski & Sacchi, 1987). cDNA was synthesised using SuperScript™II Reverse Transcriptase (Invitrogen by Thermo Fisher Scientific). The following primers were used:
mouse *Ilk* forward 5′-GTGGCTGGACAACACAGAGA-3′,
mouse *Ilk* reverse 5′-ATCCCCACGATTCATCACAT-3′,
mouse *beta-2 microglobulin (B2m)* forward 5′-GAGCCCAAGACCGTCTACTG-3′,
mouse *B2m* reverse 5′-GCTATTTCTTTCTGCGTGCAT-3′,
human *ILK* forward 5′-AAGGTGCTGAAGGTTCGAGA-3′,
human *ILK* reverse 5′-ATACGGCATCCAGTGTGTGA-3′,
human *B2M* forward 5′-TTTCATCCATCCGACATTGA-3′,
human *B2M* reverse 5′-CCTCCATGATGCTGCTTACA-3′.
Quantitative real-time PCR was performed by using the LightCycler Nano Device (Roche). All experiments were performed in duplicates or triplicates.

Statistical analysis

Statistical significance was determined by using Excel (Microsoft) or Prism software (GraphPad Inc.). Normal distribution of data was tested with the Shapiro–Wilk normality test for sample sizes of $n \geq 7$. Unpaired two-tailed Student's *t*-test (with Welch's correction) was performed for comparisons of two groups, while one-way ANOVA followed by Tukey or Dunnett post hoc test or two-way ANOVA followed by Tukey post hoc test was performed for multiple comparisons. Additional non-parametric tests were used for not normally distributed data, in particular the unpaired, two-tailed Mann–Whitney test for comparisons of two groups or the

Kruskal–Wallis test followed by Dunn's post hoc test for multiple comparisons. Differences were considered significant with a $P < 0.05$, and $P < 0.0001$ are stated as $P = 0.0001$. Quantified data are presented as means ± standard error of the mean (SEM). No statistical method was used to predetermine sample size. The experiments were not randomised, but investigators were blinded to allocation during some experiments and outcome assessment. Significant outliers were detected by the extreme studentized deviate method (Grubbs' test) for $n \geq 4$ embryos, mice or samples, and excluded from the statistical analysis. In addition, adult mice with morphological abnormalities were excluded from the statistical analysis.

Study approval

All animal experiments were approved by the local Animal Ethics Committee of the Landesamt für Natur, Umwelt und Verbraucherschutz Nordrhein-Westfalen (LANUV North Rhine-Westphalia, Germany), and conducted according to the German Animal Protection Laws.

Data availability

All data that support the conclusions are available from the corresponding author on request.

Expanded View for this article is available online.

Author contributions
SU, LP-P, LSH and EL conceptually designed this study. SU and LP-P performed most experiments. LSH performed some *in vitro* knockdown and stretch experiments as well as staining, imaging and analyses of some mouse tissues. CH and AB performed *in vivo* experiments on the mouse hearts. MK-G initiated the cornea experiments and was supervised by SMP. LS and TM provided *Prox1-CreER^{T2}* mice with corresponding protocols. BP and EM provided staged and genotyped *Tie2-Cre;Parva-loxP* embryos. EL supervised the entire project. SU and EL wrote the manuscript, and all authors read and revised the final manuscript.

Conflict of interest
The authors declare that they have no conflict of interest.

References

Achen MG, Jeltsch M, Kukk E, Makinen T, Vitali A, Wilks AF, Alitalo K, Stacker SA (1998) Vascular endothelial growth factor D (VEGF-D) is a ligand for the tyrosine kinases VEGF receptor 2 (Flk1) and VEGF receptor 3 (Flt4). *Proc Natl Acad Sci USA* 95: 548 – 553

Alam A, Herault JP, Barron P, Favier B, Fons P, Delesque-Touchard N, Senegas I, Laboudie P, Bonnin J, Cassan C, Savi P, Ruggeri B, Carmeliet P, Bono F, Herbert JM (2004) Heterodimerization with vascular endothelial growth factor receptor-2 (VEGFR-2) is necessary for VEGFR-3 activity. *Biochem Biophys Res Commun* 324: 909 – 915

Avraamides CJ, Garmy-Susini B, Varner JA (2008) Integrins in angiogenesis and lymphangiogenesis. *Nat Rev Cancer* 8: 604 – 617

Baeyens N, Nicoli S, Coon BG, Ross TD, Van den Dries K, Han J, Lauridsen HM, Mejean CO, Eichmann A, Thomas JL, Humphrey JD, Schwartz MA (2015) Vascular remodeling is governed by a VEGFR3-dependent fluid shear stress set point. *Elife* 4: e04645

Bazigou E, Xie S, Chen C, Weston A, Miura N, Sorokin L, Adams R, Muro AF, Sheppard D, Makinen T (2009) Integrin-alpha9 is required for fibronectin matrix assembly during lymphatic valve morphogenesis. *Dev Cell* 17: 175 – 186

Bazigou E, Lyons OT, Smith A, Venn GE, Cope C, Brown NA, Makinen T (2011) Genes regulating lymphangiogenesis control venous valve formation and maintenance in mice. *J Clin Invest* 121: 2984 – 2992

Bendig G, Grimmler M, Huttner IG, Wessels G, Dahme T, Just S, Trano N, Katus HA, Fishman MC, Rottbauer W (2006) Integrin-linked kinase, a novel component of the cardiac mechanical stretch sensor, controls contractility in the zebrafish heart. *Genes Dev* 20: 2361 – 2372

Choi D, Park E, Jung E, Seong YJ, Hong M, Lee S, Burford J, Gyarmati G, Peti-Peterdi J, Srikanth S, Gwack Y, Koh CJ, Boriushkin E, Hamik A, Wong AK, Hong YK (2017a) ORAI1 activates proliferation of lymphatic endothelial cells in response to laminar flow through kruppel-like factors 2 and 4. *Circ Res* 120: 1426 – 1439

Choi D, Park E, Jung E, Seong YJ, Yoo J, Lee E, Hong M, Lee S, Ishida H, Burford J, Peti-Peterdi J, Adams RH, Srikanth S, Gwack Y, Chen CS, Vogel HJ, Koh CJ, Wong AK, Hong YK (2017b) Laminar flow downregulates Notch activity to promote lymphatic sprouting. *J Clin Invest* 127: 1225 – 1240

Chomczynski P, Sacchi N (1987) Single-step method of RNA isolation by acid guanidinium thiocyanate-phenol-chloroform extraction. *Anal Biochem* 162: 156 – 159

Coon BG, Baeyens N, Han J, Budatha M, Ross TD, Fang JS, Yun S, Thomas JL, Schwartz MA (2015) Intramembrane binding of VE-cadherin to VEGFR2 and VEGFR3 assembles the endothelial mechanosensory complex. *J Cell Biol* 208: 975 – 986

Ding L, Dong L, Chen X, Zhang L, Xu X, Ferro A, Xu B (2009) Increased expression of integrin-linked kinase attenuates left ventricular remodeling and improves cardiac function after myocardial infarction. *Circulation* 120: 764 – 773

Dixelius J, Makinen T, Wirzenius M, Karkkainen MJ, Wernstedt C, Alitalo K, Claesson-Welsh L (2003) Ligand-induced vascular endothelial growth factor receptor-3 (VEGFR-3) heterodimerization with VEGFR-2 in primary lymphatic endothelial cells regulates tyrosine phosphorylation sites. *J Biol Chem* 278: 40973 – 40979

Dobreva I, Fielding A, Foster LJ, Dedhar S (2008) Mapping the integrin-linked kinase interactome using SILAC. *J Proteome Res* 7: 1740 – 1749

Dumont DJ, Jussila L, Taipale J, Lymboussaki A, Mustonen T, Pajusola K, Breitman M, Alitalo K (1998) Cardiovascular failure in mouse embryos deficient in VEGF receptor-3. *Science* 282: 946 – 949

Escobedo N, Proulx ST, Karaman S, Dillard ME, Johnson N, Detmar M, Oliver G (2016) Restoration of lymphatic function rescues obesity in Prox1-haploinsufficient mice. *JCI Insight* 1: e85096

Favier B, Alam A, Barron P, Bonnin J, Laboudie P, Fons P, Mandron M, Herault JP, Neufeld G, Savi P, Herbert JM, Bono F (2006) Neuropilin-2 interacts

with VEGFR-2 and VEGFR-3 and promotes human endothelial cell survival and migration. *Blood* 108: 1243–1250

Fraccaroli A, Pitter B, Taha AA, Seebach J, Huveneers S, Kirsch J, Casaroli-Marano RP, Zahler S, Pohl U, Gerhardt H, Schnittler HJ, Montanez E (2015) Endothelial alpha-parvin controls integrity of developing vasculature and is required for maintenance of cell-cell junctions. *Circ Res* 117: 29–40

Friedrich EB, Liu E, Sinha S, Cook S, Milstone DS, MacRae CA, Mariotti M, Kuhlencordt PJ, Force T, Rosenzweig A, St-Arnaud R, Dedhar S, Gerszten RE (2004) Integrin-linked kinase regulates endothelial cell survival and vascular development. *Mol Cell Biol* 24: 8134–8144

Galvagni F, Pennacchini S, Salameh A, Rocchigiani M, Neri F, Orlandini M, Petraglia F, Gotta S, Sardone GL, Matteucci G, Terstappen GC, Oliviero S (2010) Endothelial cell adhesion to the extracellular matrix induces c-Src-dependent VEGFR-3 phosphorylation without the activation of the receptor intrinsic kinase activity. *Circ Res* 106: 1839–1848

Garmy-Susini B, Avraamides CJ, Schmid MC, Foubert P, Ellies LG, Barnes L, Feral C, Papayannopoulou T, Lowy A, Blair SL, Cheresh D, Ginsberg M, Varner JA (2010) Integrin alpha4beta1 signaling is required for lymphangiogenesis and tumor metastasis. *Cancer Res* 70: 3042–3051

Ghatak S, Morgner J, Wickstrom SA (2013) ILK: a pseudokinase with a unique function in the integrin-actin linkage. *Biochem Soc Trans* 41: 995–1001

Gkretsi V, Apte U, Mars WM, Bowen WC, Luo JH, Yang Y, Yu YP, Orr A, St-Arnaud R, Dedhar S, Kaestner KH, Wu C, Michalopoulos GK (2008) Liver-specific ablation of integrin-linked kinase in mice results in abnormal histology, enhanced cell proliferation, and hepatomegaly. *Hepatology* 48: 1932–1941

Gousopoulos E, Proulx ST, Scholl J, Uecker M, Detmar M (2016) Prominent lymphatic vessel hyperplasia with progressive dysfunction and distinct immune cell infiltration in lymphedema. *Am J Pathol* 186: 2193–2203

Gousopoulos E, Proulx ST, Bachmann SB, Dieterich LC, Scholl J, Karaman S, Bianchi R, Detmar M (2017) An important role of VEGF-C in promoting lymphedema development. *J Invest Dermatol* 137: 1995–2004

Gu R, Bai J, Ling L, Ding L, Zhang N, Ye J, Ferro A, Xu B (2012) Increased expression of integrin-linked kinase improves cardiac function and decreases mortality in dilated cardiomyopathy model of rats. *PLoS One* 7: e31279

Hagerling R, Pollmann C, Andreas M, Schmidt C, Nurmi H, Adams RH, Alitalo K, Andresen V, Schulte-Merker S, Kiefer F (2013) A novel multistep mechanism for initial lymphangiogenesis in mouse embryos based on ultramicroscopy. *EMBO J* 32: 629–644

Hannigan GE, Leung-Hagesteijn C, Fitz-Gibbon L, Coppolino MG, Radeva G, Filmus J, Bell JC, Dedhar S (1996) Regulation of cell adhesion and anchorage-dependent growth by a new beta 1-integrin-linked protein kinase. *Nature* 379: 91–96

Harvey NL, Srinivasan RS, Dillard ME, Johnson NC, Witte MH, Boyd K, Sleeman MW, Oliver G (2005) Lymphatic vascular defects promoted by Prox1 haploinsufficiency cause adult-onset obesity. *Nat Genet* 37: 1072–1081

Henri O, Pouehe C, Houssari M, Galas L, Nicol L, Edwards-Levy F, Henry JP, Dumesnil A, Boukhalfa I, Banquet S, Schapman D, Thuillez C, Richard V, Mulder P, Brakenhielm E (2016) Selective stimulation of cardiac lymphangiogenesis reduces myocardial edema and fibrosis leading to improved cardiac function following myocardial infarction. *Circulation* 133: 1484–1497; discussion 1497

Horton ER, Byron A, Askari JA, Ng DHJ, Millon-Fremillon A, Robertson J, Koper EJ, Paul NR, Warwood S, Knight D, Humphries JD, Humphries MJ (2015) Definition of a consensus integrin adhesome and its dynamics during adhesion complex assembly and disassembly. *Nat Cell Biol* 17: 1577–1587

Huang XZ, Wu JF, Ferrando R, Lee JH, Wang YL, Farese RV Jr, Sheppard D (2000) Fatal bilateral chylothorax in mice lacking the integrin alpha9beta1. *Mol Cell Biol* 20: 5208–5215

Huang LH, Elvington A, Randolph GJ (2015) The role of the lymphatic system in cholesterol transport. *Front Pharmacol* 6: 182

Humphries JD, Byron A, Humphries MJ (2006) Integrin ligands at a glance. *J Cell Sci* 119: 3901–3903

Hynes RO (2002) Integrins: bidirectional, allosteric signaling machines. *Cell* 110: 673–687

Ishikawa Y, Akishima-Fukasawa Y, Ito K, Akasaka Y, Tanaka M, Shimokawa R, Kimura-Matsumoto M, Morita H, Sato S, Kamata I, Ishii T (2007) Lymphangiogenesis in myocardial remodelling after infarction. *Histopathology* 51: 345–353

Jeltsch M, Kaipainen A, Joukov V, Meng X, Lakso M, Rauvala H, Swartz M, Fukumura D, Jain RK, Alitalo K (1997) Hyperplasia of lymphatic vessels in VEGF-C transgenic mice. *Science* 276: 1423–1425

Joukov V, Pajusola K, Kaipainen A, Chilov D, Lahtinen I, Kukk E, Saksela O, Kalkkinen N, Alitalo K (1996) A novel vascular endothelial growth factor, VEGF-C, is a ligand for the Flt4 (VEGFR-3) and KDR (VEGFR-2) receptor tyrosine kinases. *EMBO J* 15: 1751

Kadry YA, Huet-Calderwood C, Simon B, Calderwood DA (2018) Kindlin-2 interacts with a highly-conserved surface of ILK to regulate focal adhesion localization and cell spreading. *J Cell Sci* 131: jcs221184

Kaipainen A, Korhonen J, Mustonen T, van Hinsbergh VW, Fang GH, Dumont D, Breitman M, Alitalo K (1995) Expression of the fms-like tyrosine kinase 4 gene becomes restricted to lymphatic endothelium during development. *Proc Natl Acad Sci USA* 92: 3566–3570

Karkkainen MJ, Ferrell RE, Lawrence EC, Kimak MA, Levinson KL, McTigue MA, Alitalo K, Finegold DN (2000) Missense mutations interfere with VEGFR-3 signalling in primary lymphoedema. *Nat Genet* 25: 153–159

Karkkainen MJ, Haiko P, Sainio K, Partanen J, Taipale J, Petrova TV, Jeltsch M, Jackson DG, Talikka M, Rauvala H, Betsholtz C, Alitalo K (2004) Vascular endothelial growth factor C is required for sprouting of the first lymphatic vessels from embryonic veins. *Nat Immunol* 5: 74–80

Kisanuki YY, Hammer RE, Miyazaki J, Williams SC, Richardson JA, Yanagisawa M (2001) Tie2-Cre transgenic mice: a new model for endothelial cell-lineage analysis *in vivo*. *Dev Biol* 230: 230–242

Klein KR, Caron KM (2015) Adrenomedullin in lymphangiogenesis: from development to disease. *Cell Mol Life Sci* 72: 3115–3126

Klotz L, Norman S, Vieira JM, Masters M, Rohling M, Dube KN, Bollini S, Matsuzaki F, Carr CA, Riley PR (2015) Cardiac lymphatics are heterogeneous in origin and respond to injury. *Nature* 522: 62–67

Kukk E, Lymboussaki A, Taira S, Kaipainen A, Jeltsch M, Joukov V, Alitalo K (1996) VEGF-C receptor binding and pattern of expression with VEGFR-3 suggests a role in lymphatic vascular development. *Development* 122: 3829–3837

Lange A, Wickstrom SA, Jakobson M, Zent R, Sainio K, Fassler R (2009) Integrin-linked kinase is an adaptor with essential functions during mouse development. *Nature* 461: 1002–1006

Li F, Zhang Y, Wu C (1999) Integrin-linked kinase is localized to cell-matrix focal adhesions but not cell-cell adhesion sites and the focal adhesion localization of integrin-linked kinase is regulated by the PINCH-binding ANK repeats. *J Cell Sci* 112(Pt 24): 4589–4599

Licht AH, Raab S, Hofmann U, Breier G (2004) Endothelium-specific Cre recombinase activity in flk-1-Cre transgenic mice. *Dev Dyn* 229: 312–318

Lorenz L, Axnick J, Buschmann T, Henning C, Urner S, Fang S, Nurmi H, Eichhorst N, Holtmeier R, Bodis K, Hwang JH, Mussig K, Eberhard D, Stypmann J, Kuss O, Roden M, Alitalo K, Haussinger D, Lammert E (2018)

Mechanosensing by beta1 integrin induces angiocrine signals for liver growth and survival. *Nature* 562: 128−132

Lu H, Fedak PW, Dai X, Du C, Zhou YQ, Henkelman M, Mongroo PS, Lau A, Yamabi H, Hinek A, Husain M, Hannigan G, Coles JG (2006) Integrin-linked kinase expression is elevated in human cardiac hypertrophy and induces hypertrophy in transgenic mice. *Circulation* 114: 2271−2279

Lund AW, Wagner M, Fankhauser M, Steinskog ES, Broggi MA, Spranger S, Gajewski TF, Alitalo K, Eikesdal HP, Wiig H, Swartz MA (2016) Lymphatic vessels regulate immune microenvironments in human and murine melanoma. *J Clin Invest* 126: 3389−3402

Makinen T, Veikkola T, Mustjoki S, Karpanen T, Catimel B, Nice EC, Wise L, Mercer A, Kowalski H, Kerjaschki D, Stacker SA, Achen MG, Alitalo K (2001) Isolated lymphatic endothelial cells transduce growth, survival and migratory signals via the VEGF-C/D receptor VEGFR-3. *EMBO J* 20: 4762−4773

Malan D, Elischer A, Hesse M, Wickstrom SA, Fleischmann BK, Bloch W (2013) Deletion of integrin linked kinase in endothelial cells results in defective RTK signaling caused by caveolin 1 mislocalization. *Development* 140: 987−995

Martel C, Li W, Fulp B, Platt AM, Gautier EL, Westerterp M, Bittman R, Tall AR, Chen SH, Thomas MJ, Kreisel D, Swartz MA, Sorci-Thomas MG, Randolph GJ (2013) Lymphatic vasculature mediates macrophage reverse cholesterol transport in mice. *J Clin Invest* 123: 1571−1579

Merx MW, Gorressen S, van de Sandt AM, Cortese-Krott MM, Ohlig J, Stern M, Rassaf T, Godecke A, Gladwin MT, Kelm M (2014) Depletion of circulating blood NOS3 increases severity of myocardial infarction and left ventricular dysfunction. *Basic Res Cardiol* 109: 398

Montanez E, Ussar S, Schifferer M, Bosl M, Zent R, Moser M, Fassler R (2008) Kindlin-2 controls bidirectional signaling of integrins. *Genes Dev* 22: 1325−1330

Montanez E, Wickstrom SA, Altstatter J, Chu H, Fassler R (2009) Alpha-parvin controls vascular mural cell recruitment to vessel wall by regulating RhoA/ROCK signalling. *EMBO J* 28: 3132−3144

Nikolopoulos SN, Turner CE (2000) Actopaxin, a new focal adhesion protein that binds paxillin LD motifs and actin and regulates cell adhesion. *J Cell Biol* 151: 1435−1448

Nilsson I, Bahram F, Li X, Gualandi L, Koch S, Jarvius M, Soderberg O, Anisimov A, Kholova I, Pytowski B, Baldwin M, Yla-Herttuala S, Alitalo K, Kreuger J, Claesson-Welsh L (2010) VEGF receptor 2/3 heterodimers detected *in situ* by proximity ligation on angiogenic sprouts. *EMBO J* 29: 1377−1388

Norman S, Riley PR (2016) Anatomy and development of the cardiac lymphatic vasculature: Its role in injury and disease. *Clin Anat* 29: 305−315

Nossuli TO, Lakshminarayanan V, Baumgarten G, Taffet GE, Ballantyne CM, Michael LH, Entman ML (2000) A chronic mouse model of myocardial ischemia-reperfusion: essential in cytokine studies. *Am J Physiol Heart Circ Physiol* 278: H1049−H1055

Okazaki T, Ni A, Ayeni OA, Baluk P, Yao LC, Vossmeyer D, Zischinsky G, Zahn G, Knolle J, Christner C, McDonald DM (2009) alpha5beta1 Integrin blockade inhibits lymphangiogenesis in airway inflammation. *Am J Pathol* 174: 2378−2387

Olski TM, Noegel AA, Korenbaum E (2001) Parvin, a 42 kDa focal adhesion protein, related to the alpha-actinin superfamily. *J Cell Sci* 114: 525−538

Partanen TA, Arola J, Saaristo A, Jussila L, Ora A, Miettinen M, Stacker SA, Achen MG, Alitalo K (2000) VEGF-C and VEGF-D expression in neuroendocrine cells and their receptor, VEGFR-3, in fenestrated blood vessels in human tissues. *FASEB J* 14: 2087−2096

Pasquet JM, Noury M, Nurden AT (2002) Evidence that the platelet integrin alphaIIb beta3 is regulated by the integrin-linked kinase, ILK, in a PI3-kinase dependent pathway. *Thromb Haemost* 88: 115−122

Planas-Paz L, Strilic B, Goedecke A, Breier G, Fassler R, Lammert E (2012) Mechanoinduction of lymph vessel expansion. *EMBO J* 31: 788−804

Planas-Paz L, Lammert E (2014) Mechanosensing in developing lymphatic vessels. *Adv Anat Embryol Cell Biol* 214: 23−40

Potocnik AJ, Brakebusch C, Fassler R (2000) Fetal and adult hematopoietic stem cells require beta1 integrin function for colonizing fetal liver, spleen, and bone marrow. *Immunity* 12: 653−663

Rutkowski JM, Moya M, Johannes J, Goldman J, Swartz MA (2006) Secondary lymphedema in the mouse tail: Lymphatic hyperplasia, VEGF-C upregulation, and the protective role of MMP-9. *Microvasc Res* 72: 161−171

Sabine A, Saygili Demir C, Petrova TV (2016) Endothelial cell responses to biomechanical forces in lymphatic vessels. *Antioxid Redox Signal* 25: 451−465

Sakai T, Li S, Docheva D, Grashoff C, Sakai K, Kostka G, Braun A, Pfeifer A, Yurchenco PD, Fassler R (2003) Integrin-linked kinase (ILK) is required for polarizing the epiblast, cell adhesion, and controlling actin accumulation. *Genes Dev* 17: 926−940

Salameh A, Galvagni F, Bardelli M, Bussolino F, Oliviero S (2005) Direct recruitment of CRK and GRB2 to VEGFR-3 induces proliferation, migration, and survival of endothelial cells through the activation of ERK, AKT, and JNK pathways. *Blood* 106: 3423−3431

Schulte-Merker S, Sabine A, Petrova TV (2011) Lymphatic vascular morphogenesis in development, physiology, and disease. *J Cell Biol* 193: 607−618

Serrano I, McDonald PC, Lock F, Muller WJ, Dedhar S (2013) Inactivation of the Hippo tumour suppressor pathway by integrin-linked kinase. *Nat Commun* 4: 2976

Skobe M, Hawighorst T, Jackson DG, Prevo R, Janes L, Velasco P, Riccardi L, Alitalo K, Claffey K, Detmar M (2001) Induction of tumor lymphangiogenesis by VEGF-C promotes breast cancer metastasis. *Nat Med* 7: 192−198

Soderberg O, Gullberg M, Jarvius M, Ridderstrale K, Leuchowius KJ, Jarvius J, Wester K, Hydbring P, Bahram F, Larsson LG, Landegren U (2006) Direct observation of individual endogenous protein complexes *in situ* by proximity ligation. *Nat Methods* 3: 995−1000

Srinivasan RS, Dillard ME, Lagutin OV, Lin FJ, Tsai S, Tsai MJ, Samokhvalov IM, Oliver G (2007) Lineage tracing demonstrates the venous origin of the mammalian lymphatic vasculature. *Genes Dev* 21: 2422−2432

Sweet DT, Jimenez JM, Chang J, Hess PR, Mericko-Ishizuka P, Fu J, Xia L, Davies PF, Kahn ML (2015) Lymph flow regulates collecting lymphatic vessel maturation *in vivo*. *J Clin Invest* 125: 2995−3007

Tammela T, Zarkada G, Wallgard E, Murtomaki A, Suchting S, Wirzenius M, Waltari M, Hellstrom M, Schomber T, Peltonen R, Freitas C, Duarte A, Isoniemi H, Laakkonen P, Christofori G, Yla-Herttuala S, Shibuya M, Pytowski B, Eichmann A, Betsholtz C *et al* (2008) Blocking VEGFR-3 suppresses angiogenic sprouting and vascular network formation. *Nature* 454: 656−660

Tatin F, Renaud-Gabardos E, Godet AC, Hantelys F, Pujol F, Morfoisse F, Calise D, Viars F, Valet P, Masri B, Prats AC, Garmy-Susini B (2017) Apelin modulates pathological remodeling of lymphatic endothelium after myocardial infarction. *JCI Insight* 2: 93887

Thomson BR, Heinen S, Jeansson M, Ghosh AK, Fatima A, Sung HK, Onay T, Chen H, Yamaguchi S, Economides AN, Flenniken A, Gale NW, Hong YK, Fawzi A, Liu X, Kume T, Quaggin SE (2014) A lymphatic defect

causes ocular hypertension and glaucoma in mice. *J Clin Invest* 124: 4320–4324

Traister A, Aafaqi S, Masse S, Dai X, Li M, Hinek A, Nanthakumar K, Hannigan G, Coles JG (2012) ILK induces cardiomyogenesis in the human heart. *PLoS One* 7: e37802

Tu Y, Huang Y, Zhang Y, Hua Y, Wu C (2001) A new focal adhesion protein that interacts with integrin-linked kinase and regulates cell adhesion and spreading. *J Cell Biol* 153: 585–598

Urner S, Kelly-Goss M, Peirce SM, Lammert E (2018) Mechanotransduction in blood and lymphatic vascular development and disease. *Adv Pharmacol* 81: 155–208

Vaynberg J, Fukuda K, Lu F, Bialkowska K, Chen Y, Plow EF, Qin J (2018) Non-catalytic signaling by pseudokinase ILK for regulating cell adhesion. *Nat Commun* 9: 4465

Veikkola T, Jussila L, Makinen T, Karpanen T, Jeltsch M, Petrova TV, Kubo H, Thurston G, McDonald DM, Achen MG, Stacker SA, Alitalo K (2001) Signalling via vascular endothelial growth factor receptor-3 is sufficient for lymphangiogenesis in transgenic mice. *EMBO J* 20: 1223–1231

Wang JF, Zhang XF, Groopman JE (2001) Stimulation of beta 1 integrin induces tyrosine phosphorylation of vascular endothelial growth factor receptor-3 and modulates cell migration. *J Biol Chem* 276: 41950–41957

Wang Y, Nakayama M, Pitulescu ME, Schmidt TS, Bochenek ML, Sakakibara A, Adams S, Davy A, Deutsch U, Luthi U, Barberis A, Benjamin LE, Makinen T, Nobes CD, Adams RH (2010) Ephrin-B2 controls VEGF-induced angiogenesis and lymphangiogenesis. *Nature* 465: 483–486

White DE, Coutu P, Shi YF, Tardif JC, Nattel S, St Arnaud R, Dedhar S, Muller WJ (2006) Targeted ablation of ILK from the murine heart results in dilated cardiomyopathy and spontaneous heart failure. *Genes Dev* 20: 2355–2360

Wigle JT, Oliver G (1999) Prox1 function is required for the development of the murine lymphatic system. *Cell* 98: 769–778

Wigle JT, Harvey N, Detmar M, Lagutina I, Grosveld G, Gunn MD, Jackson DG, Oliver G (2002) An essential role for Prox1 in the induction of the lymphatic endothelial cell phenotype. *EMBO J* 21: 1505–1513

Wilting J, Becker J, Buttler K, Weich HA (2009) Lymphatics and inflammation. *Curr Med Chem* 16: 4581–4592

Xu Y, Yuan L, Mak J, Pardanaud L, Caunt M, Kasman I, Larrivee B, Del Toro R, Suchting S, Medvinsky A, Silva J, Yang J, Thomas JL, Koch AW, Alitalo K, Eichmann A, Bagri A (2010) Neuropilin-2 mediates VEGF-C-induced lymphatic sprouting together with VEGFR3. *J Cell Biol* 188: 115–130

Yang Y, Garcia-Verdugo JM, Soriano-Navarro M, Srinivasan RS, Scallan JP, Singh MK, Epstein JA, Oliver G (2012) Lymphatic endothelial progenitors bud from the cardinal vein and intersomitic vessels in mammalian embryos. *Blood* 120: 2340–2348

Yuan L, Moyon D, Pardanaud L, Breant C, Karkkainen MJ, Alitalo K, Eichmann A (2002) Abnormal lymphatic vessel development in neuropilin 2 mutant mice. *Development* 129: 4797–4806

Zervas CG, Gregory SL, Brown NH (2001) *Drosophila* integrin-linked kinase is required at sites of integrin adhesion to link the cytoskeleton to the plasma membrane. *J Cell Biol* 152: 1007–1018

Zhang X, Groopman JE, Wang JF (2005) Extracellular matrix regulates endothelial functions through interaction of VEGFR-3 and integrin alpha5beta1. *J Cell Physiol* 202: 205–214

Zhang F, Zarkada G, Han J, Li J, Dubrac A, Ola R, Genet G, Boye K, Michon P, Kunzel SE, Camporez JP, Singh AK, Fong GH, Simons M, Tso P, Fernandez-Hernando C, Shulman GI, Sessa WC, Eichmann A (2018) Lacteal junction zippering protects against diet-induced obesity. *Science* 361: 599–603